UNIVERSITÀ DEGLI STUDI DI MILANO

FACOLTÀ DI SCIENZE E TECNOLOGIE

Corso di Laurea Magistrale in Fisica

Multifractal dimension of a QCD superinclusive observable

Relatore:
Prof. Stefano Forte

Correlatore:
Prof. Simone Marzani

Tesi di Laurea di:
Daniele Atzori
Matricola: **28347A**

Anno Accademico 2023-2024

Contents

Introduction

The Standard Model (SM) is a Quantum Field Theory (QFT) that describes the elementary particles and the fundamental forces between them (strong, weak and electromagnetic). According to the SM, the basic constituents of matter are spin 1/2 particles (fermions), that can be divided into quarks and leptons, considering their interactions; whereas, forces are mediated by gauge bosons, particles with integer spin. The SM is based on the following group of symmetry:

$$\mathrm{SU}(3)_C \otimes \mathrm{SU}(2)_L \otimes \mathrm{U}(1)_Y, \tag{1}$$

the first component is linked to the strong interaction, while the second and third ones are linked to the electro-weak interaction. The electromagnetic interaction is described by Quantum Electrodynamics (QED), then unified with the weak interaction in the Glashow-Salam-Weinberg theory: according to this gauge theory, leptons and quarks interact through the weak interaction, mediated by the $Z/W^{\pm}$ bosons, and the electromagnetic force, mediated by the photon (which is massless). The introduction of the Higgs boson and the so-called Higgs mechanism explain how fermions and gauge bosons can acquire mass through the spontaneous symmetry breaking (SSB) of the gauge group $\mathrm{SU}(2)_L \otimes \mathrm{U}(1)_Y$.

This thesis discusses topics in Quantum Chromodynamics (QCD), which is the theory that describes the strong interaction: the particles that interact through this force are the quarks (fermions) and the gluons (gauge bosons); these particles cannot be directly observed alone, but they only exist in bound states, called hadrons. QCD is a non-abelian gauge theory, based on the $\mathrm{SU}(3)_C$ symmetry group. An important property of QCD is the so-called asymptotic freedom: the coupling constant α_S of the strong force becomes small for high energy, in other words the strength of the interaction decreases as the energy of process increases; therefore, in the high-energy region, the theory can be treated in a perturbative way, and this leads to the so-called perturbative QCD.

Particle colliders have been and are extremely useful for the development of perturbative QCD, as they can reach very high energies: nowadays, these machines can accelerate and collide particle beams with a centre-of-mass energy up to the order of 10 TeV. The electron-positron annihilation and the deep inelastic scattering between a lepton and an hadron are two interesting processes from this point of view. In this thesis we consider an electron-positron scattering process, narrowing the focus to events with QCD final-state radiation. The analysis of hadron production in this process permits various tests of the validity of perturbative QCD, for example through the measure of the total cross section or the so-called event shape variables, quantities which characterizes the "shape" of a final-state event [1]. In 1978, Giorgio Parisi introduced the idea of a superinclusive variable [3], which is defined accepting any type of particle in the final state; however, this idea has not been much developed respect to other event shape variables, which are widely studied.

In this thesis we define and study a superinclusive observable, which allows one to study the energy flow of an event due to QCD final-state radiation. We give a theoretical prediction of its behaviour in the collinear limit, that is the limit in which angles between radiated particles are small: analytical calculations show that this observable follows a multifractal law, with a multifractal dimension that depends on the so-called anomalous dimensions of the Altarelli-Parisi splitting functions [4].

In the first chapter we will give a theoretical introduction, explaining basics of QCD, its quantization and renormalization; in the second chapter, we will analyse QCD in the infrared region, treating advanced topics like factoriazion, jets and IRC safety; in the third chapter we will talk about event shape variables and their resummation, with a particular focus on the concept of superinclusive observables; in the fourth chapter we will present the concept of multifractal. The first four chapters treat topics already known and present in the literature; the fifth chapter contains the analytical calculation that proves the multifractal law, while in the sixth chapter we will comment this result. In treating QCD topics we will mainly follow the book [1].

Chapter 1

Basics of QCD

1.1 Introduction to QCD

The fundamental quanta of QCD are quarks and gluons; hadrons are bound states of these fundamental quanta. They can be divided into mesons, made up of a quark-antiquark pair ($q\bar{q}$), and baryons, made up of three quarks (qqq). According to SM, quarks exist in six different flavours:

Flavour	Electric charge	Mass
up (u)	$+2/3$	2 MeV
down (d)	$-1/3$	5 MeV
charm (c)	$+2/3$	1.3 GeV
strange (s)	$-1/3$	130 MeV
top (t)	$+2/3$	173 GeV
bottom (b)	$-1/3$	4.2 GeV

Table 1.1: Different flavours of quark with relative masses and electric charges (in units of e).

u, d and s are called light quarks, while c, t and b heavy quarks. QCD requires the introduction of a new quantic number, the colour: quarks can exist in three different colours (red, blue and green). The hadrons observed have no colour charge, leading to the assumption that only colourless bound states of quarks can exist: this is called colour confinement.

Quantization of QCD

QCD is locally invariant under the colour group $\mathrm{SU}(3)_C$, so it is a gauge theory. We can parametrize an element of $\mathrm{SU}(3)_C$ in the following way:

$$U(x) = \exp\left\{ig\theta_a(x)t^a\right\}, \tag{1.1}$$

where t^a are the generators of the $su(3)_C$ algebra, with $a = 1, ..., N_C^2 - 1$ (N_C is the number of colours). They follow the commutation rules given by the so-called structure constants f^{abc}:

$$\left[t^a, t^b\right] = if^{ab}{}_c t^c. \tag{1.2}$$

As $SU(3)_C$ is a special unitary group, the representation for the generators t^a have to be provided by hermitian and traceless matrices. For the SM, $N_C = 3$, so a representation for the generators t^a is provided by the eight Gell-Mann matrices. The request of gauge invariance leads to the introduction of $N_C^2 - 1$ gauge fields $A_\mu^a(x)$, whose quanta are the gluons, massless spin 1 particles.

The Lagrangian of the theory is the following:

$$\mathcal{L}_{QCD} = -\frac{1}{4} F_{\mu\nu}^a F_a^{\mu\nu} + \sum_{f=1}^{N_f} \bar{\psi}_i^f \left(i \not{D}^{ij} - m_f \delta^{ij} \right) \psi_j^f, \tag{1.3}$$

where ψ_i^f are the quark fields: i is the colour index, while f represent the flavour. $F_{\mu\nu}^a$ is the gluon field strength tensor:

$$F_{\mu\nu}^a = \partial_\mu A_\nu^a - \partial_\nu A_\mu^a + g f^a{}_{bc} A_\mu^b A_\nu^c. \tag{1.4}$$

The third term shows the non abelian nature of the theory. In the Lagrangian, D_μ is the covariant derivative:

$$D_\mu^{ij} = \delta^{ij} \partial_\mu - i g A_\mu^a t_a^{ij}. \tag{1.5}$$

From Eq. (1.3) it is clear that QCD is diagonal in the flavour space: interactions that mix flavours are not allowed.

In order to perform quantization, we have to choose a gauge configuration, because we can allow the propagation of only the physical degrees of freedom of the gluon (transverse polarizations). We can impose a constraint on the gauge field maintaining the Lorentz covariance; this is the so-called Lorentz condition:

$$\partial^\mu A_\mu^a(x) = 0. \tag{1.6}$$

And then we must add a gauge-fixing term in the Lagrangian:

$$\mathcal{L}_{GF} = -\frac{1}{2\xi} (\partial^\mu A_\mu^a)^2, \tag{1.7}$$

where ξ is a Lagrange multiplier. Gauge invariance is broken at the level of the Lagrangian, but the physical results must be independent from both the gauge and the value of ξ. The non-abelian nature of the theory, so the possibility of a self-interaction of the gluon, brakes gauge invariance and unitarity of the theory; in order to avoid that, we introduce ghosts, fields that appear only in the intermediate steps of the calculation and not in the final results, cancelling the temporal and longitudinal degrees of freedom of the gluon:

$$\eta^a = \frac{1}{\sqrt{2}} (\eta_1^a + i \eta_2^a), \qquad (\eta_1^a)^2 = (\eta_2^a)^2 = 0. \tag{1.8}$$

Their dynamics is described by the Fadeev-Popov Lagrangian:

$$\mathcal{L}_{FP} = \partial_\mu \eta^{a\dagger} D_{ab}^\mu \eta^b. \tag{1.9}$$

From the Lagrangian given by $\mathcal{L}_{QCD} + \mathcal{L}_{GF} + \mathcal{L}_{FP}$, we can write down the Feynman rules and the expressions of the propagators; the form of the gluon propagator depends on the gauge. Besides the covariant gauge, another choice we could make is the physical gauge, in which we choose a frame, characterized by a vector n, and we identify the physical degrees of freedom from the beginning. In this case, the gauge condition is the following:

$$n^\mu A^a_\mu(x) = 0. \tag{1.10}$$

1.2 Asymptotic freedom

1.2.1 Renormalization of QCD and the running coupling constant

In QFT, radiative corrections lead to divergences in calculations. Ultraviolet divergences are treated with renormalization. The renormalization procedure substitutes the bare (non-physical) parameters of the Lagrangian with new renormalized quantities, related to the physical observables; it develops into three steps:

- regularization of the diverging integrals;
- subtraction of the contributes that diverge;
- cancellation of these contributes through the redefinition of the bare parameters.

't Hooft and Veltman showed that every Yang-Mills theory (like QCD) is renormalizable order by order in perturbation theory: every ultraviolet divergence can be treated with the redefinition of a finite number of parameters.

This procedure introduces an arbitrary energy scale μ, called renormalization scale: it defines the point at which the subtractions are performed and it is a non-physical parameter. A consequence of renormalization is the introduction of a running coupling constant: we can understand this considering a dimensionless physical observable R; being Q the energy of the process, we would say that R does not depend on Q: in fact, after providing a series expansion, R depends on powers of Q, but, having Q the dimension of an energy and being R dimensionless, it can depend only on Q^0, so it does not depend on Q; however, this is not true in a renormalizable quantum field theory: if we calculate R as a perturbation series of $\alpha_S = g^2/4\pi$, the renormalization procedure introduces the energy scale μ, so R depends in general on the ratio Q^2/μ^2 (since R is dimensionless) and also the coupling constant α_S depends on the choice of μ [1]. However, R is a physical observable, while μ is an arbitrary quantity, so R cannot depend on μ; mathematically, the total derivative of R with respect to μ must be zero, so we obtain the renormalization group equation (RGE):

$$\mu^2 \frac{d}{d\mu^2} R\left(Q^2/\mu^2, \alpha_S(\mu^2)\right) \equiv \left[\mu^2 \frac{\partial}{\partial \mu^2} + \mu^2 \frac{\partial \alpha_S}{\partial \mu^2} \frac{\partial}{\partial \alpha_S}\right] R = 0. \tag{1.11}$$

In order to solve this equation, we can define the following quantities [1]:

$$t \equiv \log \frac{Q^2}{\mu^2}, \qquad \beta(\alpha_S) \equiv \mu^2 \frac{\partial \alpha_S}{\partial \mu^2}. \tag{1.12}$$

Then, Eq. (1.11) becomes

$$\left[-\frac{\partial}{\partial t} + \beta(\alpha_S)\frac{\partial}{\partial \alpha_S}\right] R(e^t, \alpha_S) = 0. \tag{1.13}$$

We can solve this partial differential equation by implicitly defining the so-called running coupling constant $\alpha_S(Q^2)$:

$$t \equiv \int_{\alpha_S}^{\alpha_S(Q^2)} \frac{dx}{\beta(x)}, \qquad \text{where} \quad \alpha_S \equiv \alpha_S(\mu^2). \tag{1.14}$$

We obtain the following equations by differentiating Eq. (1.14):

$$\frac{\partial \alpha_S(Q^2)}{\partial t} = \beta(\alpha_S(Q^2)), \qquad \frac{\partial \alpha_S(Q^2)}{\partial \alpha_S} = \frac{\beta(\alpha_S(Q^2))}{\beta(\alpha_S)}. \tag{1.15}$$

Now, it should be clear that $R(1, \alpha_S(Q^2))$ is a solution of Eq. (1.11); this means that the scale dependence in a dimensionless quantity like R enters only through the running of the coupling constant: so, if we calculate the quantity $R(1, \alpha_S)$ in fixed-order perturbation theory, we can predict the variation of R with Q only by solving Eq. (1.15) [1].

1.2.2 Asymptotic freedom

We found that, after the renormalization procedure, the coupling constant depends on the energy scale of the process. This dependence is described by the renormalization group equation (1.15).

In perturbation theory, the function β has an expansion in series:

$$\beta(\alpha_S) = -\sum_{n=2}^{+\infty} \beta_{n-2}\alpha_S^n = -\beta_0\alpha_S^2 - \beta_1\alpha_S^3 - \beta_2\alpha_S^4 - ... \tag{1.16}$$

The coefficients of (1.16) are obtained from the higher-order loop corrections to the bare vertices of the theory. If we are in a small-coupling region, we can consider only the first term of the expansion and the RGE becomes

$$\frac{\partial}{\partial \log Q^2}\alpha_S(Q^2) = -\beta_0\alpha_S^2(Q^2) + \mathcal{O}(\alpha_S^3), \tag{1.17}$$

solution of which is given by the following expression:

$$\alpha_S(Q^2) = \frac{\alpha_S(\mu^2)}{1 + \beta_0\alpha_S(\mu^2)\log\frac{Q^2}{\mu^2}}. \tag{1.18}$$

In QED, the value of β_0 is extracted from the self-energy of the photon, obtaining

$$\beta_0^{QED} = -\frac{1}{3\pi} < 0. \tag{1.19}$$

A negative value of β_0 means that the coupling increases as the energy increases. In QCD, this value is extracted form the self-energy of the gluon, which is given by two diagrams: one with a quark loop and the other with a gluon loop; the latter is a consequence of the non-abelian nature of QCD (in fact, we have not a diagram of this type in QED). We obtain

$$\beta_0^{QCD} = \frac{1}{12\pi}(11N_C - 2N_f), \qquad \beta_0^{QCD} > 0 \Leftrightarrow N_f \leq 16. \tag{1.20}$$

As $N_f = 6$, β_0^{QCD} is positive: so, contrary to QED, in QCD the coupling is small at high energies. This behaviour is called asymptotic freedom and it implies that at high energies we can treat particles as weakly interacting and perform calculations following a perturbative approach.

The one-loop expression of the running coupling constant (1.18) diverges at a certain energy scale Λ^2_{QCD}, that satisfies the following relation:

$$1 + \beta_0 \alpha_S(\mu^2) \log \frac{\Lambda^2_{QCD}}{\mu^2} = 0. \tag{1.21}$$

Λ_{QCD} is called Landau pole or fundamental scale of the QCD and is given by the following formula (at one loop):

$$\Lambda_{QCD} = \mu \exp \left\{ -\frac{1}{2\beta_0 \alpha_S(\mu^2)} \right\}. \tag{1.22}$$

Substituting this relation in Eq. 1.18, we obtain the following expression for the running coupling constant:

$$\alpha_S(Q^2) = \frac{1}{\beta_0 \log \frac{Q^2}{\Lambda^2_{QCD}}}. \tag{1.23}$$

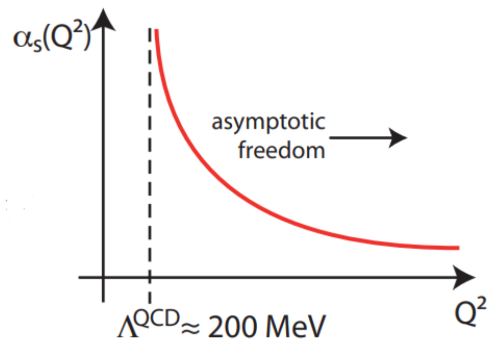

Figure 1.1: Running coupling constant of the strong interaction.

1.3 Hard scattering and perturbative QCD

Hard-scattering processes have an energy scale $Q \gg m_p$, where m_p is the mass of the proton. In this energy region asymptotic freedom is valid, because $\alpha_S(Q^2) \ll 1$, so we can consider hadrons as made of weakly-interacting particles, called partons (quarks and gluons), and calculate cross sections at partonic leve using a perturbative approach. However, due to the confinement, the states predicted by the theory are the hadrons. At this point, we have two possibilities:

- if we do not have hadrons in the initial state, we can sum over all final states and obtain the total cross section with a perturbative partonic calculation;
- if we have hadrons in the initial state, we can use a property called factorization and calculate the total hadronic cross section as a convolution of the partonic cross section and the so-called PDFs, which will be defined later.

Now, we will briefly present these two possibilities with two scattering processes: the electron-positron annihilation, which is the process we will consider to define the observable in Chapter 5, and the deep inelastic scattering, whose study will lead us to introduce the PDFs, the Altarelli-Parisi splitting functions and the Altarelli-Parisi evolution equation.

1.3.1 Electron-positron annihilation

In this process, an electron and a positron annihilate producing a virtual boson (a photon γ or a Z), which decays (at lowest order) in a fermion-antifermion pair.

In this thesis we are interested in higher-order QCD corrections of this process, given by the emission of virtual or real partons; we indicate the order of these corrections as Next-to-Leading-Order (NLO), Next-to-Next-to-Leading-Order (NNLO) and so on; the N^{n}LO contribution is of order $\alpha_S^n(Q^2)$. We can calculate the total cross section in a perturbative way and sum over all possible final states.

In the perturbative QCD picture, particle masses smaller than Λ_{QCD} are zero: so light quarks are massless; however, heavy quarks masses can be neglected in the hard-scattering regime. So, from now on, we will consider every particle massless. We will made a further assumption: we will suppose that the energy is far below the Z peak ($\Lambda_{QCD} \ll Q \ll M_Z$, $M_Z \simeq 91.2\,\text{GeV}$), so that we can neglect the Z channel and take into account only the production of a virtual photon.

The Feynman diagram of the process at LO is represented in the following picture:

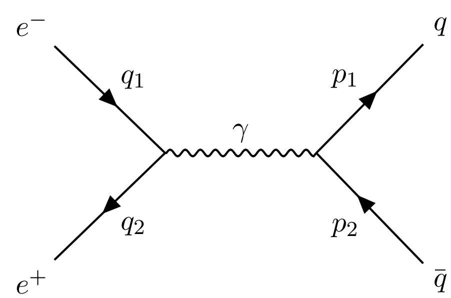

Figure 1.2: Feynman diagram of the process at LO.

The squared modulus of the amplitude is given by the following formula [2]:

$$|\bar{\mathcal{M}}_{LO}|^2 = \frac{8e^4 e_q^2}{Q^4}\left[(q_1 \cdot p_1)(q_2 \cdot p_2) + (q_1 \cdot p_2)(q_2 \cdot p_1)\right], \tag{1.24}$$

where e_q is the electric charge of the quark in terms of e, the electric charge of the electron. Summing over all kinematically accessible flavours and colours the differential cross section with respect to the centre-of-mass scattering angle θ of the final state quark is given by the following formula:

$$\frac{d\sigma}{d\cos\theta} = \frac{\pi\alpha^2}{2Q^2} N_C(1+\cos^2\theta)\sum_q e_q^2, \tag{1.25}$$

where α is the fine-structure constant of the QED and the sum over q has to be interpreted as a sum over the quark flavours. Integrating over θ, we obtain the total cross section at Born level:

$$\sigma_0 = \frac{4\pi\alpha^2}{3Q^2} N_C \sum_q e_q^2. \tag{1.26}$$

At NLO, we have both real and virtual contributions to the total cross section.

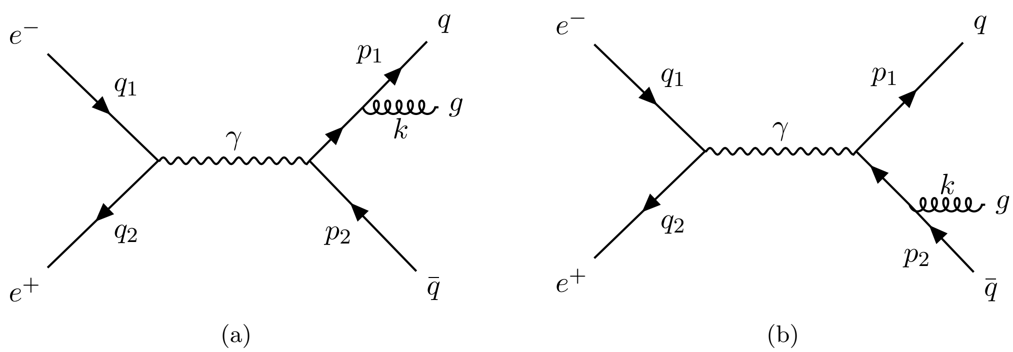

Figure 1.3: Feynman diagrams of real gluon emissions at NLO.

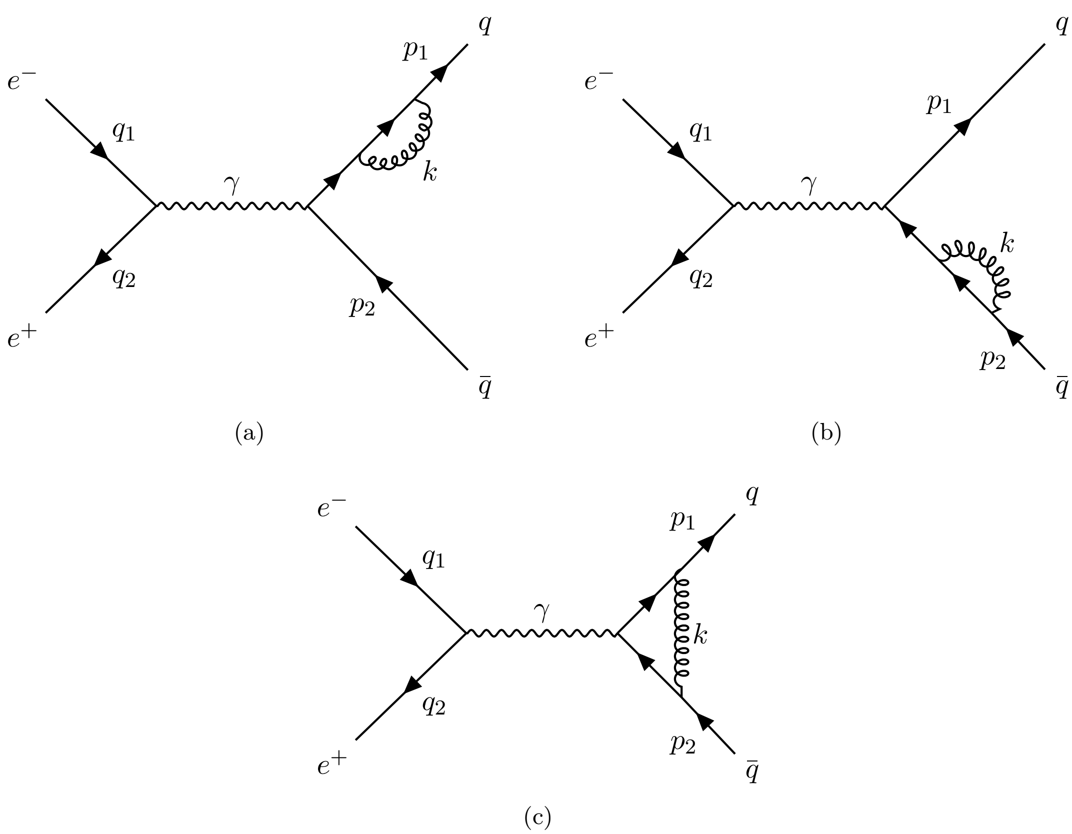

Figure 1.4: Feynman diagrams of virtual gluon emissions at NLO.

The matrix element for the real gluon emission process is given by the following formula:

$$\frac{1}{4}|\bar{\mathcal{M}}_{q\bar{q}g}|^2 = 24C_F e^4 e_q^2 g_S^2 \frac{(p_1 \cdot q_1)^2 + (p_1 \cdot q_2)^2 + (p_2 \cdot q_1)^2 + (p_2 \cdot q_2)^2}{(q_1 \cdot q_2)\,(p_1 \cdot k)\,(p_2 \cdot k)}, \tag{1.27}$$

where $C_F = \frac{4}{3}$ is a constant related to the $su(3)$ algebra, while $g_S^2 = 4\pi\alpha_S$.

In order to calculate the cross section, it is useful to introduce the following quantities:

$$x_1 = \frac{2E_q}{Q}, \qquad x_2 = \frac{2E_{\bar{q}}}{Q}, \tag{1.28}$$

where E_q and $E_{\bar{q}}$ are the energies of the quark and the antiquark, respectively. Introducing the Euler angles α, β and γ, the three-body phase space integration can be written as

$$d\phi_3 = \frac{1}{(2\pi)^5}\frac{Q^2}{32} d\alpha d\cos\beta d\gamma dx_1 dx_2. \tag{1.29}$$

The total cross section for the real emission is given by the following integral [1]:

$$\sigma_{q\bar{q}g} = \sigma_0 \cdot 3\sum_q e_q^2 \int dx_1 dx_2 C_F \frac{\alpha_S}{2\pi}\frac{x_1^2 + x_2^2}{(1-x_1)(1-x_2)}. \tag{1.30}$$

The integration region is $0 \leq x_1, x_2 \leq 1$, $x_1 + x_2 \geq 1$. It is clear that the integral 1.30 is divergent in the limits $x_i \to 1$. It can be shown that the quantities x_i are related to the energy of the gluon (E_3) and the angles between the gluon and the quarks (named θ_{13} and θ_{23} respectively):

$$1 - x_1 = \frac{x_2 E_3}{Q}\left(1 - \cos\theta_{23}\right), \tag{1.31}$$

$$1 - x_2 = \frac{x_1 E_3}{Q}\left(1 - \cos\theta_{13}\right). \tag{1.32}$$

This means that the integral is divergent in the regions of the phase space where the gluon is collinear with the quark or the antiquark ($\theta_{i3} \to 0, i = 1, 2$) or where the emitted gluon is soft ($E_3 \to 0$). However, it can be proved that these infrared divergences don't constitute a problem: in fact, if we regularize the integral (1.30) and consider the contributions given by the virtual gluon emissions, the divergences cancel and the final result is finite:

$$\sigma = \sigma_0 \left\{1 + \frac{\alpha_S}{\pi} + \mathcal{O}\left(\alpha_S^2\right)\right\}. \tag{1.33}$$

So, it happens that IR loop-integral divergences and IR phase-space divergences cancel. The cancellation of infrared singularities in perturbative theory is stated by the Bloch-Nordsieck (BN) theorem for Quantum Electrodynamics alone and by the Kinoshita-Lee-Naunberg (KLN) theorem for the whole Standard Model.

In the next chapter we will treat soft and collinear emissions in detail, introducing the Altarelli-Parisi splitting functions, fundamental tools for the purpose of this thesis.

1.3.2 Deep inelastic scattering

The deep inelastic scattering is the collision between a lepton and a hadron, so, contrary to the electron-positron annihilation, it is a scattering process with hadrons in initial state.

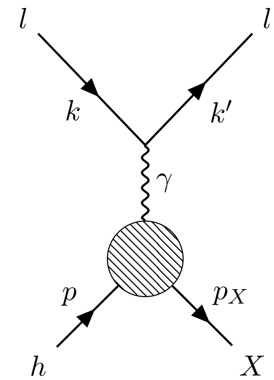

Figure 1.5: Feynman diagram of the deep inelastic scattering.

Where l is a lepton and X is any hadronic final state (inclusivity). In this case, we have higher-order QCD corrections also to the initial state:

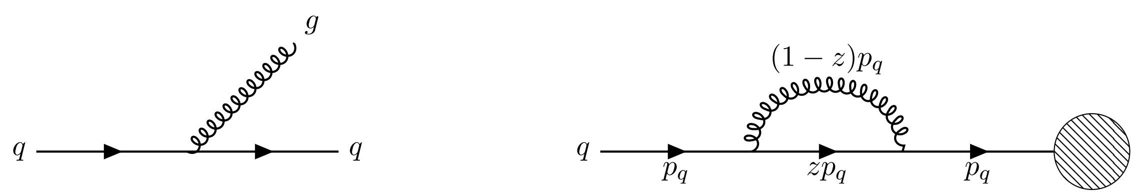

Figure 1.6: Higher-order corrections to partons in initial state; p_q is the momentum of a parton inside the hadron.

In the last section we saw that higher-order corrections give rise to infrared divergences, that cancel if we accept any possible final state; however, we cannot be inclusive on the initial state, so divergences due to initial-state emissions have to be treated differently.

We begin by defining some variables [1]:

$$q^\mu = k^\mu - k'^\mu, \tag{1.34}$$
$$Q^2 = -q^2, \tag{1.35}$$
$$m_h^2 = p^2, \tag{1.36}$$
$$\nu = p \cdot q = M(E' - E), \tag{1.37}$$
$$x = \frac{Q^2}{2\nu} = \frac{Q^2}{2M(E - E')}, \tag{1.38}$$
$$y = \frac{q \cdot p}{k \cdot p} = 1 - \frac{E'}{E}, \tag{1.39}$$

where q is the momentum transfer, m_h is the hadron mass and E, E' are the energies of l, l' respectively, in the proton rest frame.

The scattering is said inelastic if $m_X^2 > m_h^2$, deep inelastic if $m_X^2 \gg m_h^2$; we are working in the hard-scattering regime.

We assume that $l = e$. As for the electron-scattering annihilation, we consider only the exchange of a virtual photon. In order to calculate the cross section, we can divide the problem into two levels:

- leptonic: interaction between the electron and the virtual photon;
- hadronic: interaction between the virtual photon and the hadron.

The hadronic level is treated by introducing the so-called hadronic structure functions $F_i\left(x, Q^2\right)$ $(i = 1, 2)$, which parametrize the structure of the hadron target as "seen" by the photon [1]. Without neglecting the hadron mass, the total hadronic cross section is given by the following formula:

$$\begin{aligned}\frac{d^2\sigma}{dxdy} \quad &= \quad \frac{8\pi\alpha^2 m_h E}{Q^4}\left[\left(\frac{1+(1-y)^2}{2}\right)2xF_1(x,Q^2)\right.\\ &\left. +(1-y)\left(F_2(x,Q^2)-2xF_1(x,Q^2)\right)-\frac{M}{2E}xyF_2(x,Q^2)\right]. \qquad (1.40)\end{aligned}$$

If we consider also the coupling with the Z and $W^{\pm}$ bosons, the cross section will contain an additional term with a third structure function $F_3\left(x, Q^2\right)$, which violates parity.

In the Bjorken limit, i.e. $Q, \nu \to +\infty$ with x fixed, the structure functions obey an approximate scaling law (see Chapter 4) and are observed to depend only on x:

$$F_i(x, Q^2) \to F_i(x). \qquad (1.41)$$

Bjorken scaling means that the photon scatters off point-like constituents of the hadron: in fact, the dimensionless structure functions can depend only on the ratio Q/Q_0, where $1/Q_0$ is a length scale characterizing the constituents, which does not exist if they are point-like [1].

If we study the process in a frame where the hadron is moving very fast, we can say that the photon scatters off a quark constituent of the hadron, moving parallel with it and carrying a fraction z of its momentum, $p_q = zp$. If we neglect the hadron mass, the total hadronic cross section becomes

$$\frac{d^2\sigma}{dxdQ^2} = \frac{4\pi\alpha}{Q^4}\left[\left[1+(1-y)^2\right]F_1\left(x,Q^2\right)+\frac{1-y}{x}\left(F_2\left(x,Q^2\right)-2xF_1\left(x,Q^2\right)\right)\right], \qquad (1.42)$$

Starting from the matrix element of the process $e^+e^- \to q\bar{q}$, we can obtain the matrix element for the process $e^-q \to e^-q$ and the partonic cross section for the process:

$$\frac{d\hat{\sigma}}{dQ^2} = \frac{2\pi\alpha^2 e_q^2}{Q^4}\left[1+(1-y)^2\right]. \qquad (1.43)$$

The mass-shell constraint for the outgoing quark is

$$p_q'^2 = (p_q+q)^2 = q^2 + 2p_q \cdot q = -2p \cdot q(x-z) = 0, \qquad (1.44)$$

which means that $x = z$. We can write the double differential cross section for the partonic scattering process:

$$\frac{d^2\hat{\sigma}}{dxdQ^2} = \frac{4\pi\alpha^2}{Q^4}\left[1+(1-y)^2\right]\frac{1}{2}e_q^2\delta(x-z). \tag{1.45}$$

If we introduce the partonic structure functions $\hat{F}_i\left(x, Q^2\right)$, we can write down the following relation:

$$F_{i,h}(x,Q^2) = \sum_a \int_0^1 dz f_{a,h}(z)\hat{F}_i(\hat{x},Q^2), \tag{1.46}$$

where $\hat{x} = x/z$ and $f_{a,h}(z)$ is called parton density function (PDF) and indicates the probability of finding a parton a inside the hadron h carrying a fraction z of its momentum. According to Eq. (1.46), the DIS can be interpreted as the scattering between the virtual photon and the partons, each with a specific probability.
By comparing Eq. (1.42) and Eq. (1.45), we can see that at LO

$$\hat{F}_2 = xe_a^2\delta(x-z) = 2x\hat{F}_1, \tag{1.47}$$

which leads to the following relations:

$$\begin{cases} F_{2,h}(x) = x\sum_a e_a^2 f_{a,h}(x) \\ 2xF_{1,h}(x) = F_2(x) \end{cases} \tag{1.48}$$

The second result is known as Callan-Gross relation, it is a consequence of the fact that quarks are spin-$\frac{1}{2}$ particles, so they cannot absorb a vector boson with longitudinal polarization. Sometimes, instead of F_1 and F_2 the so-called longitudinal structure function is used:

$$F_L(x,Q^2) = \left(1+\frac{4m_h^2x^2}{Q^2}\right)F_2(x,Q^2) - 2xF_1(x,Q^2) \underset{Q^2\to+\infty}{\longrightarrow} F_2(x) - 2xF_1(x), \tag{1.49}$$

which is identically zero in the Bjorken limit.

Higher-orders QCD corrections to the initial state introduce infrared divergences, which are treated through the renormalization of the PDFs. The procedure is equal to the UV renormalization:

- we notice that the introduced PDFs are bare quantities $f_{a,h}^{(0)}(z)$;
- we reabsorb the singularities by redefining the PDFs.

The renormalization procedure introduces an arbitrary scale, called factorization scale μ_F^2, which indicates the point at which the redefinition is performed. This introduces an energy-dependence of the PDFs:

$$f_{a,h}^{(0)}(z) \Rightarrow f_{a,h}\left(z,\mu_F^2\right). \tag{1.50}$$

At this point, we can calculate the parton cross section in perturbative theory and convolute it with the PDFs to obtain the hadronic cross section:

$$\sigma_h(Q^2) = \sum_a \int_0^1 dz f_{a,h}(z, \mu_F^2) \hat{\sigma}_a(z, \alpha_S(Q^2), \mu_F^2, Q^2). \tag{1.51}$$

Eq. (1.51) is called factorization formula. The PDFs and the parton cross section depend on the factorization scale μ_F^2, while the hadronic cross section depends only on the energy of the process Q^2.

PDFs can't be theoretically calculated, but they have to be determined in experiments; however, their scale dependence is given by the Altarelli-Parisi evolution equation, which will be presented in the next chapter.

Chapter 2

QCD in the infrared region

2.1 Soft and collinear splitting

In the previous chapter we saw that matrix elements which involve massless particles may exhibit infrared divergences in the soft and collinear limits. These divergences appear in the calculations as large logarithms: these terms will have a crucial role in the study of the superinclusive observable (Chapter 5). Soft singularities occur in correspondence of the emission or the exchange of particles with vanishing four-momentum, in the presence of massless vector bosons (such as gluons); these divergences may occur also if the matter particles are massive. Collinear divergences are due to the splitting of particles at small angles and occur only in the presence of massless particles [7]. In the presence of massive particles, the large logarithms are still present but not diverging.

Starting from Eq. (1.30), we will see that in the collinear and soft limits the cross section factorizes and the splitting are represented by universal factors, which do not depend on the process. We have the following result for the matrix element $|\mathcal{M}_{real}|^2$ of the process $e^+e^- \to q\bar{q}g$:

$$|\mathcal{M}_{real}|^2 \propto \frac{x_1^2 + x_2^2}{(1-x_1)(1-x_2)}. \tag{2.1}$$

With some trivial algebra, it can be shown that

$$\frac{x_1^2 + x_2^2}{(1-x_1)(1-x_2)} = \frac{1-(1-x_3)^2}{x_3}\left(\frac{1}{1-x_1} + \frac{1}{1-x_2}\right) - 2. \tag{2.2}$$

Hence, the amplitude contains the sum of two independent soft and collinear contributions and a finite term, which originates from the interference of the two diagrams in Fig. 1.3.

The total cross section is obtained by integrating the matrix element over the phase space, with the constraint $x_1 + x_2 + x_3 = 2$:

$$\sigma_{q\bar{q}g} = \int dx_1 dx_2 dx_3 \delta(x_1 + x_2 + x_3 - 2)|\mathcal{M}_{real}|^2. \tag{2.3}$$

It follows that, in the soft and collinear limits, each diagram give an independent contribution to the total cross section, which is proportional to the Born cross section. For example, the contribution given by the emission of a real gluon from the antiquark (diagram (b) in Fig. 1.3) is

$$\sigma_0 \frac{dx_1 dx_3}{1-x_1} \frac{1+(1-x_3)^2}{x_3} = \sigma_0 \frac{d\cos\theta_{23}}{1-\cos\theta_{23}} dx_3 P_{qq}(x_3). \tag{2.4}$$

We introduced the so-called Altarelli-Parisi splitting function:

$$P_{qq}(x_3) \equiv C_F \frac{\alpha_S}{2\pi} \frac{1+(1-x_3)^2}{x_3}. \tag{2.5}$$

The contribution given by diagram (a) in Fig. 1.3 has the same form of Eq. (2.4), with $1 \leftrightarrow 2$. We have to sum both the contributions to obtain the total cross section; the interference of the two diagrams is negligible. Hence, we say that a cross section factorizes in the presence of a splitting if it is equal to the convolution of the lower order cross section and a correction that states the probability of the splitting.

In Eq. (2.4) it is clear that the physics factorizes: this happens because the emissions of soft and collinear gluons occur at a much longer time than the production of the quark-antiquark pair, so the interference between these processes is negligible in this limit. This is an heuristic explanation of the factorization.

This can be generalized. Let us assume that the final state of a process contains $m+1$ particles: if the i-th is soft or is collinear to the j-th particle, the Born-level matrix element $|\mathcal{M}^{(\text{tree})}_{m+1}|^2$ is equal to the matrix element of a process with m particle $|\mathcal{M}^{(\text{tree})}_{m}|^2$, where the particles i and j are substituted by an unique particle with momentum given by the sum of their momenta $p_i + p_j$, all multiplied by a universal function V_{ij}.

$$|\mathcal{M}^{(\text{tree})}_{m+1}(p_1, ..., p_i, ..., p_j, ..., p_{m+1})|^2 \sim |\mathcal{M}^{(\text{tree})}_{m}(p_1, ..., p_i + p_j, ..., p_m)|^2 \cdot V_{ij}. \tag{2.6}$$

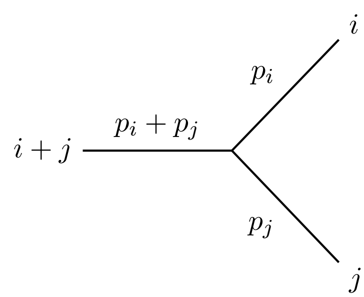

Figure 2.1: Splitting.

Let θ_{ij} be the splitting angle and z the fraction of momentum carried by the particle i: so $p_i = z(p_i + p_j)$ and $p_j = (1-z)(p_i + p_j)$; if the splitting is collinear, the function V_{ij} is

$$V_{ij} = \frac{1}{\theta_{ij}^2} P_{ij}(z), \tag{2.7}$$

where $P_{ij}(z)$ is the Altarelli-Parisi splitting function.
The infrared factorization is valid also for the emission of a virtual particle; if $\mathcal{M}^{(\text{1-loop})}_{m}(\{p_i\})$ is the 1-loop amplitude, we have the following result:

$$\mathcal{M}^{(\text{1-loop})}_{m}(p_1, ..., p_m)\mathcal{M}^{(\text{tree})*}_{m}(p_1, ..., p_m) + h.c. \sim -|\mathcal{M}^{(\text{tree})}_{m}(p_1, ..., p_m)|^2 \int_{loop} V_{ij}. \tag{2.8}$$

2.1.1 The Altarelli-Parisi splitting functions

We introduced the Altarelli-Parisi (AP) splitting functions: these are universal functions that state the probability of a collinear splitting with a fraction z of momentum transferred. These functions can be calculated in perturbative QCD and don't depend on the process we are studying.

In general, $P_{ab}(z)$ indicates the probability of the parton evolution $b(p) \to a(zp)$ and it has the following structure:

$$P_{ab}(z) = \left(\frac{\alpha_S}{2\pi}\right) P_{ab}^{(0)}(z) + \left(\frac{\alpha_S}{2\pi}\right)^2 P_{ab}^{(1)}(z) + \left(\frac{\alpha_S}{2\pi}\right)^3 P_{ab}^{(2)}(z) + \left(\frac{\alpha_S}{2\pi}\right)^4 P_{ab}^{(3)}(z) + \mathcal{O}(\alpha_S^5). \tag{2.9}$$

The function in Eq. (2.5) is the LO term of the Altarelli-Parisi function for the emission of a real gluon carrying a fraction $x_3 \equiv 1 - z$ of the initial momentum:

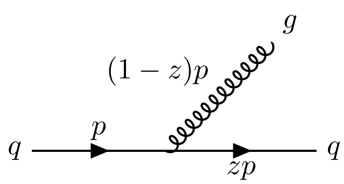

$$\Longrightarrow \qquad \left[P_{qq}^{(0)}\right]_{real} = C_F \frac{1+z^2}{1-z}$$

Figure 2.2: Real emission of a gluon from a quark and related AP function at lowest order.

It is clear that this function diverges in the limit $z \to 1$, when the emitted gluon is soft. This happens because we are not considering the emission of a virtual gluon, whose AP function at LO is the following:

$$\left[P_{qq}^{(0)}(z)\right]_{virt.} = -\lim_{\epsilon\to 0} \delta(1-z) \int_0^1 dz' \left[P_{qq}^{(0)}(z')\right]_{real} \Theta(1 - z' > \epsilon). \tag{2.10}$$

The ϵ parameter plays the role of an infrared cut-off. Summing the real and virtual contributions, we obtain the AP function at LO for the process $q(p) \to q(zp) + g((1-z)p)$:

$$P_{qq}^{(0)}(z) = C_F \left[\frac{1+z^2}{(1-z)_+} + \frac{3}{2}\delta(1-z)\right], \tag{2.11}$$

where the plus distribution is defined as follows:

$$\frac{1}{(1-z)_+} = \lim_{\epsilon\to 0} \left[\frac{1}{1-z}\Theta(1 - z > \epsilon) - \delta(1-z) \int_0^{1-\epsilon} dz' \frac{1}{1-z'}\right]. \tag{2.12}$$

Acting on a smooth function $f(z)$, the distribution give the following result:

$$\int_0^1 dz f(z) \frac{1}{(1-z)_+} = \lim_{\epsilon\to 0} \int_0^{1-\epsilon} dz \frac{f(z) - f(1)}{1-z}. \tag{2.13}$$

According to the Feynman rules of QCD, we have four possible splittings:

$$q \to q + g \quad : \quad P_{qq}^{(0)}(z) = C_F \left[\frac{1+z^2}{(1-z)_+} + \frac{3}{2}\delta(1-z) \right], \tag{2.14}$$

$$g \to g + g \quad : \quad P_{gg}^{(0)}(z) = 2C_A \left[\frac{z}{(1-z)_+} + \frac{1-z}{z} + z(1-z) \right] + \frac{1}{6}\delta(1-z)(11C_A - 2N_f), \tag{2.15}$$

$$g \to q + q \quad : \quad P_{qg}^{(0)}(z) = T_R \left[z^2 + (1-z)^2 \right], \tag{2.16}$$

$$q \to g + q \quad : \quad P_{gq}^{(0)}(z) = C_F \left[\frac{1+(1-z)^2}{z} \right]. \tag{2.17}$$

2.1.2 The Altarelli-Parisi evolution equations

We already saw that higher-order corrections to initial-state partons in deep inelastic scattering break the Bjorken scaling and introduce a dependence of the parton densities on the energy scale: the AP splitting functions govern this dependence through the AP evolution equations [4].

The emission of a gluon gives the following correction to the structure function (for the complete calculation see [1]):

$$\hat{F}_2(x, Q^2) = e_q^2 x \left[\delta(1-x) + \frac{\alpha_S}{2\pi} \left(P_{qq}(x) \log \frac{Q^2}{\kappa^2} + C_q(x) \right) \right], \tag{2.18}$$

where $C_q(x)$ is a calculable function and κ is a collinear cut-off. So, beyond leading order, the Bjorken scaling is broken by logarithms of Q^2. The parton density is

$$q(x) = \delta(1-x) + \frac{\alpha}{2\pi} \left(P_{qq}(x) \log \frac{Q^2}{\kappa^2} + C_q(x) \right). \tag{2.19}$$

The cut-off is necessary as the matrix element is divergent in the collinear limit and we can't be inclusive on the initial state, because the virtual photon can distinguish a quark from a collinear quark-gluon pair [1]. The hadron structure function F_2 is given by the convolution of the quark structure function $\hat{F}_2$ with a bare distribution $q^{(0)}$, summed over quark flavours:

$$F_2(x, Q^2) = x \sum_q e_q^2 \left[q^{(0)}(x) + \frac{\alpha_S}{2\pi} \int_x^1 \frac{dz}{z} q^{(0)}(z) \left\{ P_{qq}\left(\frac{x}{z}\right) \log \frac{Q^2}{\kappa^2} + C_q\left(\frac{x}{z}\right) \right\} + ... \right]. \tag{2.20}$$

As done for the ultraviolet renormalization, we absorb the singularities into the bare distribution, introducing the so-called factorization scale μ_F^2 . This procedure redefines the PDF:

$$q(x, \mu_F^2) = q^{(0)}(x) + \frac{\alpha_S}{2\pi} \int_x^1 \frac{dz}{z} q^{(0)}(z) \left\{ P_{qq}\left(\frac{x}{z}\right) \log \frac{\mu_F^2}{\kappa^2} + C_q\left(\frac{x}{z}\right) \right\} + ... \tag{2.21}$$

The structure function becomes

$$F_2(x, Q^2) = x \sum_q e_q^2 \int_x^1 \frac{dz}{z} q(z, \mu^2) \left\{ \delta\left(1 - \frac{x}{z}\right) + \frac{\alpha_S}{2\pi} P_{qq}\left(\frac{x}{z}\right) \log \frac{Q^2}{\mu_F^2} + ... \right\}. \tag{2.22}$$

Considering all the possible splitting and introducing the gluon density g, Eq. (2.21) becomes

$$\begin{aligned} q(x,\mu_F^2) &= q^{(0)}(x) + \frac{\alpha_S}{2\pi}\int_x^1 \frac{dz}{z} q^{(0)} \left\{ P_{qq}\left(\frac{x}{z}\right)\log\frac{\mu_F^2}{\kappa^2} + C_q\left(\frac{x}{z}\right)\right\} \\ &\quad + \frac{\alpha_S}{2\pi}\int_x^1 \frac{dz}{z} g^{(0)}(z) \left\{ P_{qg}\left(\frac{x}{z}\right)\log\frac{\mu_F^2}{\kappa^2} + C_g\left(\frac{x}{z}\right)\right\} + ..., \end{aligned} \tag{2.23}$$

The scale dependence of the PDFs is given by the Altarelli-Parisi evolution equations, which are obtained taking the partial derivative with respect to $\log\mu_F^2$ of Eq. (2.22):

$$\mu_F^2 \frac{\partial}{\partial \mu_F^2} q(x,\mu_F^2) = \frac{\alpha_S(\mu_F^2)}{2\pi}\int_x^1 \frac{dz}{z} P_{qq}\left(\frac{x}{z}\right) q(x,\mu_F^2). \tag{2.24}$$

A more complete derivation, based on the operator product expansion and renormalization group methods [5, 6] extends the result to higher orders, introducing a dependence of the AP functions on the running coupling constant:

$$\mu_F^2 \frac{\partial}{\partial \mu_F^2} q(x,\mu_F^2) = \frac{\alpha_S(\mu_F^2)}{2\pi}\int_x^1 \frac{dz}{z} P_{qq}\left(\frac{x}{z}, \alpha_S(\mu_F^2)\right) q(x,\mu_F^2). \tag{2.25}$$

However, this result is valid only for non-singles distributions, i.e. differences between quark distributions, $q_{NS} = q_i - q_j$. In general, the AP evolution equation is a $(2N_f+1)$-dimensional matrix equation:

$$\mu_F^2 \frac{\partial}{\partial \mu_F^2} \begin{pmatrix} q_i(x,\mu_F^2) \\ g(x,\mu_F^2) \end{pmatrix} = \frac{\alpha_S(\mu_F^2)}{2\pi} \sum_q \int_x^1 \frac{dz}{z} \mathcal{P}\left(\frac{x}{z}, \alpha_S(\mu_F^2)\right) \begin{pmatrix} q_i(x,\mu_F^2) \\ g(x,\mu_F^2) \end{pmatrix}, \tag{2.26}$$

where

$$\mathcal{P}\left(\frac{x}{z}, \alpha_S(\mu_F^2)\right) = \begin{pmatrix} P_{q_iq_j}\left(\frac{x}{z}, \alpha(\mu_F^2)\right) & P_{q_ig}\left(\frac{x}{z} . \alpha_S(\mu_F^2)\right) \\ P_{gq_j}\left(\frac{x}{z}, \alpha(\mu_F^2)\right) & P_{gg}\left(\frac{x}{z}, \alpha(\mu_F^2)\right) \end{pmatrix}. \tag{2.27}$$

The indices i and j run over quarks and antiquarks of all flavours. The fact that colour and flavour commute has the following consequences:

$$P^{(0)}_{q_iq_j} = \delta_{ij} P^{(0)}_{qq}, \tag{2.28}$$

$$P^{(0)}_{gq_i} = P^{(0)}_{gq}, \tag{2.29}$$

$$P^{(0)}_{q_ig} = P^{(0)}_{qg}. \tag{2.30}$$

Eq. (2.28) means that the emission of a gluon does not change the flavour of a quark; Eq. (2.29) indicates that the probability of emission of a gluon is the same for all flavours, while Eq. (2.30) states that the creation of a quark-antiquark pair from a gluon has the same probability for all flavours; Eq. (2.29) and Eq. (2.30) are valid only in the massless limit. These relations clearly simplify the matrix; however, they are valid only at LO.

The interpretation of the AP functions as probabilities leads to the following sum rules:

$$\int_0^1 dx P_{qq}^{(0)}(x) = 0, \tag{2.31}$$

$$\int_0^1 dx x \left[P_{qq}^{(0)}(x) + P_{gq}^{(0)}(x)\right] = 0, \tag{2.32}$$

$$\int_0^1 dx x \left[2N_f P_{qg}^{(0)}(x) + P_{gg}^{(0)}\right] = 0. \tag{2.33}$$

where Eq. (2.31) is the baryonic number conservation, while Eq. (2.32) and Eq. (2.33) are the momentum conservation in the splitting of quarks and gluons respectively.

If we sum all the quark distributions we obtain the singlet distribution:

$$\Sigma(x, \mu_F^2) \equiv \sum_i \left[q_i(x, \mu_F^2) + \bar{q}_i(x, \mu_F^2)\right]. \tag{2.34}$$

The matrix for the singlet quark and the gluon is the following:

$$\mathcal{P}(z) \equiv \begin{pmatrix} P_{qq}(z) & 2N_f P_{qg}(z) \\ P_{gq}(z) & P_{gg}(z) \end{pmatrix}. \tag{2.35}$$

Using a matrix formalism, we can calculate the evolution probability of a general state, represented by a unit vector $v = (a, b)$, which represent a singlet quark if $a = 1$ and $b = 0$, a gluon if $a = 0$ and $b = 1$, or, in general, a superposition of the quark and gluon states if $a \neq 0, 1$ and $b \neq 0, 1$. The state after the splitting is given by the action of the Altarelli-Parisi splitting matrix $\mathcal{P}_{ij}(z)$ on the initial state vector v_i:

$$\mathcal{P}_{ij}(z)v^j = \begin{pmatrix} P_{qq}(z) & 2N_f P_{qg}(z) \\ P_{gq}(z) & P_{gg}(z) \end{pmatrix} \cdot \begin{pmatrix} a \\ b \end{pmatrix} = \begin{pmatrix} aP_{qq}(z) + 2bN_f P_{qg}(z) \\ aP_{gq}(z) + bP_{qq}(z) \end{pmatrix}. \tag{2.36}$$

In Chapter 5 we will use this formalism, summing the terms of the final vector, since we will not distinguish between quarks and gluons in the final state.

Following a different approach [4], we can provide an alternative formulation of the AP evolution equations in terms of the so-called Mellin moments of the parton distributions:

$$M_a^n(\mu_F^2) = \int_0^1 dx x^{n-1} f_a(x, \mu_F^2), \tag{2.37}$$

and the so-called anomalous dimensions of the splitting functions:

$$\gamma_{ab}^n(\alpha(\mu_F^2)) = \int_0^1 dx x^{n-1} P_{ab}(x, \alpha_S(\mu_F^2)). \tag{2.38}$$

For the non-singlet distribution the equation is

$$\mu_F^2 \frac{\partial}{\partial \mu_F^2} M_{NS}^n(\mu_F^2) = \frac{\alpha_S(\mu_F^2)}{2\pi} \gamma_{qq}^n(\alpha_S(\mu_F^2)) M_{NS}^n(\mu_F^2), \tag{2.39}$$

For the singlet quark and gluons distributions we have

$$\mu_F^2 \frac{\partial}{\partial \mu_F^2} \begin{pmatrix} M_\Sigma^n(\mu_F^2) \\ M_g^n(\mu_F^2) \end{pmatrix} = \frac{\alpha(\mu_F^2)}{2\pi} \gamma^n(\alpha_S(\mu_F^2)) \begin{pmatrix} M_\Sigma^n(\mu_F^2) \\ M_g^n(\mu_F^2) \end{pmatrix}, \tag{2.40}$$

where

$$\gamma^n = \begin{pmatrix} \gamma_{qq}^n & 2N_f\gamma_{qg}^n \\ \gamma_{gq}^n & \gamma_{gg}^n \end{pmatrix}. \tag{2.41}$$

2.1.3 Soft emission: eikonal factorization

In the caso of a soft emission, which is a particular case of the collinear emission, the matrix element factorizes. As done in the references [7, 8], we will show this property considering the matrix element of the diagram (a) in Fig. 1.3 in the limit where the emitted gluon is soft ($k \to 0$):

$$\begin{aligned} M_3^{(a)} &= g_s \bar{u}(p_1)\gamma^\mu \epsilon_\mu^*(k) \frac{\not{p}_1 + \not{k}}{(p_1+k)+i\epsilon} t_1^a \tilde{M}_2 \\ &\underset{k\to 0}{\longrightarrow} g_s \bar{u}(p_1)\gamma^\mu \epsilon_\mu^*(k) \frac{\not{p}_1}{2p_1\cdot k + i\epsilon} t_1^a \tilde{M}_2 \\ &= g_s \frac{p_1^\mu}{p_1 \cdot k} \epsilon_\mu^*(k) \bar{u}(p_1) t_1^a \tilde{M}_2, \end{aligned} \tag{2.42}$$

where we have used anti-commutation relations of the Dirac matrices and the massless Dirac equation $\not{p}_1 u(p_1) = 0$. $\tilde{M}_2$ is the LO amplitude ($e^+e^- \to q\bar{q}$) without the Dirac spinor $\bar{u}(p_1)$; $\epsilon_\mu(k)$ is the polarization vector of the emitted gluon; t_1^a is a generator of SU(3) in the fundamental representation, it's the colour charge associated to the emission of a gluon off a quark line. The factor $p_1^\mu/(p_1 \cdot k)$ in the last line of Eq. (2.42) is called eikonal factor.
Now we can calculate the squared amplitude:

$$|M_3|^2 = |M_3^{(a)} + M_3^{(b)}|^2 \underset{k\to 0}{\longrightarrow} g_s^2 \frac{p_1\cdot p_2}{(p_1\cdot k)(p_2 \cdot k)} \mathrm{Tr}\left[C_{12}\bar{u}(p_1)\tilde{M}_2\tilde{M}_2^* v(p_2)\right], \tag{2.43}$$

where we have introduce the effective colour charge:

$$C_{ij} = -2t_i^a t_j^a. \tag{2.44}$$

It can be shown that $C_{12} = 2C_F$. Thus, in the end we obtain the following factorization:

$$|M_3|^2 \underset{k\to 0}{\longrightarrow} g_s^2 2C_F \frac{p_1\cdot p_2}{(p_1\cdot k)(p_2\cdot k)} |M_2|^2 \tag{2.45}$$

$$= g_s^2 J^\mu(k) J^\nu(k)(-g_{\mu\nu}), \tag{2.46}$$

where, in the last line, we have written the matrix element in term of the *eikonal current*:

$$J^\mu(k) = \sum_{i=1}^{2} t_n^a \frac{p_n^\mu}{p_n \cdot k}. \tag{2.47}$$

2.2 IRC safety

The concepts of IRC safety is crucial to study the sensitivity of theoretical predictions to soft and collinear high-orders correction.

In perturbative QCD, we can write down the general expression of an observable:

$$\sigma = \sigma_{LO} + \sigma_{NLO} + \sigma_{NNLO} + ... \tag{2.48}$$

The prediction at LO has the following structure:

$$\sigma_{LO} = \int d\phi_m \left|\mathcal{M}_m^{(\text{tree})}(\{p_i\})\right|^2 F_m(\{p_i\}), \tag{2.49}$$

where $d\phi_m$ is the m particles phase space and $F_m(\{p_i\})$ is a function that defines the observable. At NLO we have contribution from real (first integral) and virtual (second integral) emissions:

$$\begin{aligned}\sigma_{NLO} \quad = \quad & \int d\phi_{m+1} \left|\mathcal{M}_{m+1}^{(\text{tree})}(\{p_i\})\right|^2 F_{m+1}(\{p_i\}) \\ & + \int d\phi_m \left[\mathcal{M}_m^{(\text{1-loop})}(\{p_i\})\mathcal{M}_m^{(\text{tree})*}(\{p_i\}) + c.c.\right] F_m(\{p_i\}),\end{aligned} \tag{2.50}$$

Recalling Eqs. (2.6) and (2.8), we obtain the following result:

$$\sigma_{NLO} \sim \text{F.T.} + \sum_{i,j} \int d\phi_{m+1} \left|\mathcal{M}_{m+1}^{(\text{tree})}(\{p_i\})\right|^2 \int_{loop} V_{ij} \left[F_{m+1}(..., p_i, ..., p_j, ...) - F_m(..., p_i + p_j, ...)\right], \tag{2.51}$$

where F.T. stands for finite terms in the IR limit.

In order to guarantee the complete cancellation of infrared singularities, the observable satisfy the property of IRC safety, defined as follows:

$$\begin{aligned} \text{collinear safety :} \quad & F_{m+1}(..., p_i, ..., p_j, ...) \longrightarrow F_m(..., p_i + p_j, ...) \quad \text{if } p_i \parallel p_j \\ \text{infrared safety :} \quad & F_{m+1}(..., p_i, ...) \longrightarrow F_m(..., p_{i-1}, p_{i+1}, ...) \quad \text{if } p_i \to 0 \end{aligned} \tag{2.52}$$

So, we require that whenever a parton is split into two collinear partons or a soft parton is emitted, the value of the observable must remain unchanged [8]. It should be clear that quantities made out of linear sums of momenta will respect this requirement [1]. If a variable does not satisfy this property, so it is IRC unsafe, we have to consider long-distance physics corrections, which cannot be treated with a perturbative approach. Although from an experimental point of view the finite resolution of detectors acts as a cut-off and ensures the absence of infrared singularities, we require IRC safety because we would like to avoid theoretical predictions from depending on resolutions parameters of detectors [7].

The concept of IRC safety can be generalized to every observable. An observable is said IRC safe if its theoretical prediction is insensitive to soft and collinear emissions.

2.3 Jets

In order to identify and study hadronic final states, we would like to use IRC safe definitions and observables: for this purpose, the concepts of jet and jet cross section have been introduced.

Final-state partons in high-energy scattering processes will undergo successive branchings at small angles [8], until they reach a non-perturbative energy scale and so will form hadrons. Hence, high-energy partons will appear in the final state of a collision as a collimated bunch of hadrons: these are called jets. As defined in [8], "jets are collimated flows of hadrons and they can be seen as proxies to the high-energy quarks and gluons produced in a collision".

Although in our calculation we will not identify jets, in this section we will briefly present some basic concepts.

2.3.1 Jet algorithms

In order to identify jets, we should be able to say whether two partons belongs or not to the same jets, i.e. whether two partors are collinear or not. Hence, we introduce a jet definition, which gives us an objective procedure to do that. A jet definition contains a jet algorithm and a set of parameters. In addition, a recombination scheme specifies how to obtain the kinematic properties of the jet from its components.

The so-called Snowmass accord listed five fundamental criteria that should be satisfied by any jet algorithm [8]. The algorithm should

- be simple to implement in an experimental analysis;
- be simple to implement in the theoretical calculation;
- be defined at any order in perturbation theory;
- yield finite cross sections at any order in perturbation theory;
- yield a cross section which is relatively insensitive to hadronisation.

Historically, the first IRC safe jet definition is the 2-jet rate definition, provided by Sterman and Weinberg. According to their picture, a final state is classified as a two-jet-like event if all but a fraction ϵ of the total energy is contained in a pair of cones of half-angle δ [1]. It's clear that the definition depends on the choice of the parameters ϵ and δ: this is a common feature of all the jet definitions.

Clustering algorithms

A widely-used type of algorithm is the clustering algorithm, which is based on the definition of a distance d_{ij} between two partons in the final state; starting from d_{ij}, we can define a dimensionless distance $y_{ij} = d_{ij}/Q^2$ (where Q is the energy scale of the process); after that, we introduce a dimensionless resolution parameter y_{cut}: if $y_{ij} < y_{cut}$, we recombine the partons i and j, typically by summing their momenta $p_{ij} = p_i + p_j$. Starting from calculating all the distances between the final-state partons, the procedure is repeated until $y_{ij} > y_{cut}$ for all i, j.

The algorithm depend on the choice of definition of the distance d_{ij}. For the Jade algorithm it is defined in the following way:

$$d^J_{ij} \equiv 2E_iE_j(1 - \cos\theta_{ij}). \tag{2.53}$$

This algorithm is not insensitive to non-perturbative effects (so it does not meet the fifth point of the Snowmass accord): in fact, if two partons are soft, the algorithm will cluster them even if they are not collinear.

Most of the widely-used clustering algorithms belong to the family of the generalized-k_T algorithm; this is based on the definition of a inter-particles distance d_{ij} and a beam distance d_{iB}:

$$d_{ij} = \min(k_{T,i}^{2p}, k_{T,j}^{2p})\Delta R_{ij}^2, \qquad\qquad d_{iB} = k_{T,i}^{2p} R^2, \tag{2.54}$$

where p is a free parameter, ΔR_{ij}^2 is the geometrical distance in the rapidity-azimuthal angle plane and R is a parameter called jet radius. Iteratively we compute all the d_{ij} and d_{iB}: if the smallest distance is a d_{ij}, we cluster the particles i and j; instead, if the smallest distance is a d_{iB}, object i is identified as a jet and removed from the list [8].

The value of p determines the characteristics of the algorithm. For example, the k_T algorithm correspond to $p = 1$ and it tends to cluster soft emitted partons. With $p = 0$ we obtain the Cambridge/Aachen algorithm: it is insensitive to soft emissions, as the distance is purely geometrical. The Anti-k_T algorithm correspond to $p = -1$ and has the feature that hard partons are favoured to cluster.

In the study of the jet substructure, several algorithms are used. Initially, jets are usually identified using the Anti-k_T algorithm and then the substructure is studied reclustering the components of a jet with other algorithms.

Cone algorithms

Another type of algorithm is the cone algorithm, which is based on the concept of stable cone: for a given cone centre (y_c, ϕ_c) in the rapidity-azimuth plane, if we sum the four-momenta of all the particles within a fixed radius R around the cone centre and the sum has rapidity y_c and azimuth ϕ_c, which means that the total four-momentum points in the direction of the centre of the cone, the cone is said stable. The cone algorithm starts with a given set of seeds; using them as candidates for cone centres, we calculate the cone contents and find a new centre based on the sum of the four-momenta, iteratively until we found a stable cone. It is worthy to specify that finding cones is different from finding jets, since cone can overlap; commonly, after identifying the cones, we can identify jets by merging or splitting the cones using an appropriate split-merge procedure.

2.3.2 Jet cross section

The total cross section calculated in Sect. 1.3.1 doesn't give any information about the distribution of the hadrons in the final state. After providing a jet definitions, we can calculate the jet cross section σ_n, which is the cross section for the production of n jets in the final state, and the rate $R_n \equiv \sigma_n/\sigma_{tot}$. To be useful, a jet cross section calculated in perturbative QCD should be free of soft and collinear singularities and relatively insensitive to non-perturbative corrections [1]. The Sterman-Weinberg cross section at LO coincides with the total cross section, while at NLO is calculated by integrating the matrix element in Eq. (1.27) over the phase space region where $E_i < \epsilon\sqrt{s}$ and $\theta_{ij} < \delta$; alternatively, we can subtract the three-jets cross section from the total cross section:

$$\sigma_2 = \sigma_{LO} + \sigma_{q\bar{q}g}(E_i < \epsilon\sqrt{s}, \theta_{ij} < \delta) + ... \tag{2.55}$$

$$= \sigma_{tot} - \sigma_{q\bar{q}g}(E_i > \epsilon\sqrt{s}, \theta_{ij} > \delta). \tag{2.56}$$

The cross section in Eq. (2.56) can be calculated integrating the matrix element in the phase-space region R obtained removing the infrared region from the whole phase space:

$$\sigma_{q\bar{q}g}(E_i > \epsilon\sqrt{s}, \theta_{ij} > \delta) = \int_R dx_1 dx_2 \frac{d^2\sigma_{q\bar{q}g}}{dx_1 dx_2}. \tag{2.57}$$

The final result for the rate is the following:

$$R_2 \equiv \frac{\sigma_2}{\sigma_{tot}} = 1 - \frac{4}{3}\frac{\alpha_S}{\pi}\left[4\log\delta\left(\log 2\epsilon + \frac{3}{4}\right) - \frac{5}{2} + \frac{\pi^2}{6}\right]. \tag{2.58}$$

In order to avoid infrared singularities, ϵ and δ should not be chosen too small.

In general, small values of the resolution parameters facilitate the identification of a large number of jets in the final states, as it can be seen in the following plot, provided by the OPAL collaboration:

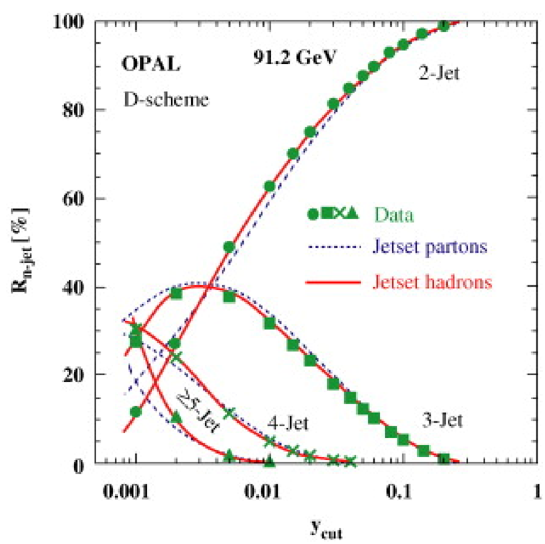

Figure 2.3: Rates of n-jet events ($2 \leq n \leq 5$) for different values of the resolution parameter y_{cut}, as measured at the Z^0 resonance at LEP [9].

Chapter 3

Event shape variables and superinclusive obervables

3.1 Event shape variables

A useful approach to study the characteristics of a hadronic final state is to use the so-called event shape variables [1]. These quantities characterize the ”shape” of an event, describing the distribution of hadrons in final states. After defining the variable X, we can give a theoretical prediction of the distribution $d\sigma/dX$ and compare it with experimental measurements.

An example of a broadly-used event shape variable is the thrust T:

$$T_m = \max_{|\boldsymbol{n}|=1} \frac{\sum_{i=1}^{m} |\boldsymbol{p_i} \cdot \boldsymbol{n}|}{\sum_{i=1}^{m} |\boldsymbol{p_i}|} \tag{3.1}$$

where $\boldsymbol{p_i}$ are the final-state parton (or hadron) momenta and $\boldsymbol{n}$ is an arbitrary unit vector. The thrust is a variable that maximizes the longitudinal momentum of an event, it takes values in the interval $(1/2, 1)$; $T = 1/2$ and $T = 1$ are two limit values:

- $T = \dfrac{1}{2}$: we have a spherical event, where all the particles are distributed isotropically;
- $T = 1$: we have a pencil-like event, with two back-to-back particles (or jets).

In the previous chapter we introduced the concept of IRC safety; this can be generalized to the event shape variables: a variable is infrared safe if it is insensitive to soft and collinear emissions. The thrust is an infrared safe variable. It is clear that it satisfies soft safety: in fact, if $p_i \to 0$, then $T_{m+1} \to T_m$. For two collinear partons with momenta $p_i = zp$ and $p_j = (1-z)p$, in the numerator of Eq. (3.1) we have

$$|\boldsymbol{p_i} \cdot \boldsymbol{n}| + |\boldsymbol{p_j} \cdot \boldsymbol{n}| = (z + 1 - z)\, |\boldsymbol{p} \cdot \boldsymbol{n}| = |(\boldsymbol{p_i} + \boldsymbol{p_j}) \cdot \boldsymbol{n}|\,, \tag{3.2}$$

whereas in the denominator

$$|\boldsymbol{p_i}| + |\boldsymbol{p_j}| = (z + 1 - z)\, |\boldsymbol{p}| = |\boldsymbol{p_i} + \boldsymbol{p_j}|\,, \tag{3.3}$$

so T is collinear safe.

Using Eq. (2.50), with $F_m = \delta(T - T_m)$, we can calculate the thrust distribution. At NLO the result is

$$\frac{1}{\sigma}\frac{d\sigma}{dT} = C_F \frac{\alpha_S}{2\pi}\left[\frac{2(3T^2-3T+2)}{T(1-T)}\log\left(\frac{2T-1}{1-T}\right) - \frac{3(3T-2)(2-T)}{1-T}\right]. \tag{3.4}$$

The distribution diverges as $T \to 1$; however, IRC safety permits us to integrate it in the interval $1/2 \leq T \leq 1$ in order to obtain the total cross section.

It is interesting to compute the expectation value $\langle 1-T \rangle$ with respect to the c.o.m. energy $\sqrt{s}$; we note that it decreases as the energy increases, which means that $\langle T \rangle \to 1$ as $\sqrt{s} \to +\infty$: in fact, if the energy is large, $\alpha_S \to 0$, so the thrust reaches the value it would have in absence of higher-order correction, which is 1, because in the final state we have only the quark-antiquark pair. In this way, it should be clear that we can provide a determination of α_S by measuring the distance of T from 1. According to this result, it can be shown that

$$\frac{1}{\sigma}\frac{d\sigma}{dT} \longrightarrow \delta(1-T) \qquad \text{if } \sqrt{s} \to +\infty. \tag{3.5}$$

Another example of an event shape is the spherocity, defined in the following way:

$$S_m = \left(\frac{4}{\pi}\right)^2 \min_{\boldsymbol{n}} \left(\frac{\sum_{i=1}^m |\boldsymbol{p_i} \times \boldsymbol{n}|}{\sum_{i=1}^m |\boldsymbol{p_i}|}\right)^2. \tag{3.6}$$

A widely-used event shape variable, which is similar to the observable we will define in Chapter 5, is the energy-energy correlation function (EEC). This quantity is a dimensionless angular distribution, defined in the following way:

$$\begin{aligned}\frac{1}{\sigma}\frac{d\Sigma}{d\cos\chi} \quad &= \quad \sum_{i\neq j}\int \frac{d^3p_i}{E_i}\frac{d^3p_j}{E_j}\left(\frac{2E_iE_j}{s}\right)E_iE_j\frac{d^6\sigma}{d^3p_id^3p_j}\delta(\cos\theta_{ij}-\cos\chi) \\ &\quad + \sum_i \int \frac{d^3p_i}{E_i}\left(\frac{E_i^2}{s}\right)E_i\frac{d^3\sigma}{d^3p_i}\delta(1-\cos\chi), \end{aligned} \tag{3.7}$$

where $E_1E_2d^6\sigma/d^3p_1d^3p_2$ is the two-hadron inclusive cross section and θ_{ij} is the angle between particles i and j. The first sum is over all distinct pairs of final-state partons (or hadrons), while the second is a self-correlation, which guarantees the validity of the following sum rule:

$$\int_{-1}^{1} d\cos\chi \frac{1}{\sigma}\frac{d\Sigma}{d\cos\chi} = 1. \tag{3.8}$$

The EEC measures the correlation of the energy flow in an event [1]. It is peaked at $\chi = 0$ and $\chi = \pi$ for a pencil-like event and it becomes flatter for a more isotropic event. It can be shown that the EEC is IRC safe.

3.1.1 Inclusive and superinclusive observables

We have already mentioned the concept of inclusivity while treating electron-positron annihilation. High-energy scattering processes produce a large multiplicity of particles and we could be interested in a particular final state, for example we could require the presence of a jet: we are inclusive if we accept any possible final state which includes the particle we are interested in.

Thus, an example of an inclusive observable is the 1-jet inclusive cross section, which measures the cross section for the production of one jet and any other particle.

In Chapter 1 we saw that the total hadronic cross section in electron-positron annihilation is free of soft and collinear singularities, as we sum over all possible final states. In 1978, before the introduction of the concept of IRC safety, G. Parisi generalized the idea of the total hadronic cross section introducing the concept of superinclusivity [3]: a superinclusive observable is defined accepting any possible final state, with no restrictions; hence, the definition of such a variable is based on a property of the final state and not on the type of particles. A superinclusive variable is free of soft and collinear singularities and can be calculated in perturbative theory at partonic level.

The example proposed by Parisi in [3] is the following 3×3 matrix:

$$\theta_{ij} = \sum_k \frac{p_i^{(k)} p_j^{(k)}}{\left|p^{(k)}\right|}, \tag{3.9}$$

where $i, j = 1, 2, 3$ and $p_i^{(k)}$ are the spatial components of the k-th particle in the centre-of-mass frame.

From Eq. (3.9) we can define the superinclusive cross section $d\sigma/d\theta_{ij}$, which can be written also in terms of the normalized eigenvalues $\lambda_1, \lambda_2, \lambda_3$ of the matrix:

$$\frac{d^3\sigma}{d\lambda_1 d\lambda_2 d\lambda_3} = \sigma(\lambda)\delta(\lambda_1 + \lambda_2 + \lambda_3 - 1). \tag{3.10}$$

From the eigenvalues of the matrix, we can define the C and D parameters:

$$C = 3(\lambda_1\lambda_2 + \lambda_2\lambda_3 + \lambda_1\lambda_3), \qquad D = 27\lambda_1\lambda_2\lambda_3. \tag{3.11}$$

This parameters are linked to the geometry of the final state, because the eigenvalues of the observable have a geometrical meaning: if only one of them is not zero, the final state consist of two jets and all the momenta are collinear; if only one eigenvalue is equal to zero, there are at least three jets and all the momenta belong to the same plane; if all the eigenvalues are equal to 1/3, the momenta distribution is completely spherical.

The C-parameter can be rewritten in terms of the final-state momenta:

$$C = \frac{3}{2} \frac{\sum_{i,j} \left[|\boldsymbol{p_i}| \, |\boldsymbol{p_j}| - (\boldsymbol{p_i} \cdot \boldsymbol{p_j})^2 / |\boldsymbol{p_i}| \, |\boldsymbol{p_j}| \right]}{\left(\sum_i |\boldsymbol{p_i}|\right)^2}. \tag{3.12}$$

3.1.2 Parton-hadron duality and the observable R

In the hard scattering regime non-perturbative hadronization effects can be neglected, this leads to the notion of parton-hadron duality: an observable has this property if experimental hadronic measurements are compatible with theoretical partonic calculations.

An example of a superinclusive observable for which the parton-hadron duality is valid is the ratio R of the total hadronic cross section to the muon pair production cross section in electron-positron annihilation [1]:

$$R = \frac{\sigma(e^+e^- \to \text{hadrons})}{\sigma(e^+e^- \to \mu^+\mu^-)} \tag{3.13}$$

This is a superinclusive observable because we accept any possible QCD final state. It can be calculated in perturbative QCD at partonic level; at LO the prediction is obtained computing the quark-antiquark pair production cross section and summing over quarks flavours and colours:

$$R_{LO} = \frac{\sum_q \sigma(e^+e^- \to q\bar{q})}{\sigma(e^+e^- \to \mu^+\mu^-)} = 3\sum_q e_q^2. \tag{3.14}$$

Using Eq. (1.33), we can include higher-order QCD corrections, obtaining the following result:

$$R = 3\sum_q e_q^2 \left\{1 + \frac{\alpha_S}{\pi} + \mathcal{O}(\alpha_S^2)\right\}. \tag{3.15}$$

Looking at the plot in Fig. 3.1, we can observe the parton-hadron duality of this observable. The theoretical prediction is compatible with the experimental data in the region $\sqrt{s} > 1$, where the perturbative approach is a valid; the discrepancies are due to the presence of resonances in the experimental data, which represent excited states of hadrons; for high energies, these resonances form a continuum, so the compatibility with the theoretical prediction increases.

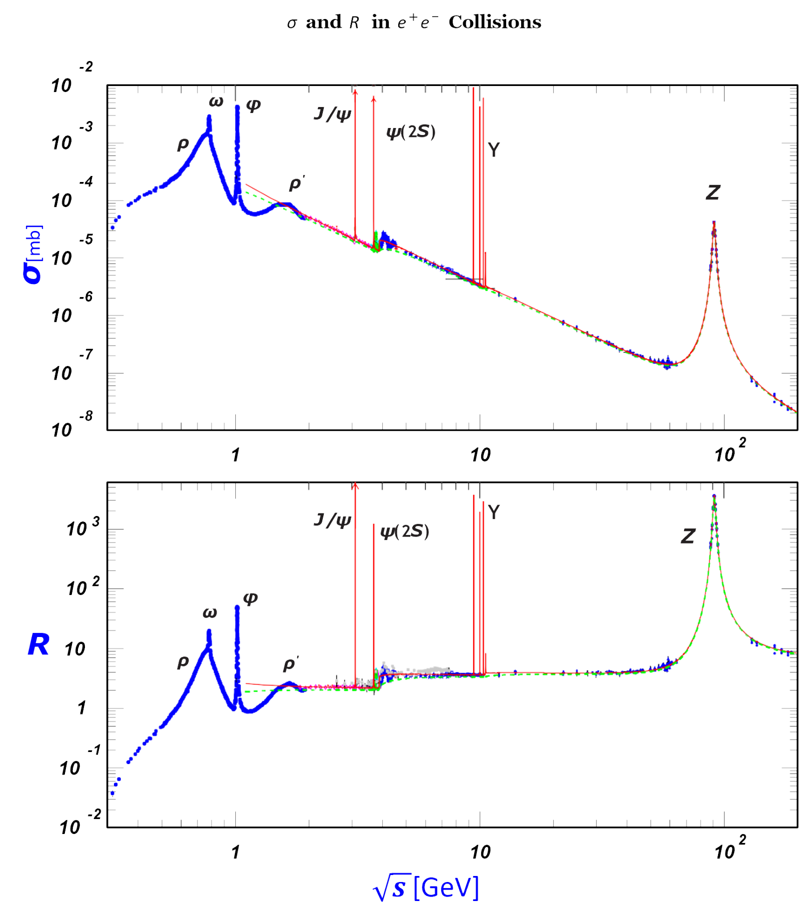

Figure 3.1: World data on the total cross section σ and the ratio R in electron-positron annihilation [10]; the broken lines represent the prediction given by the naive quark model approximation, while the solid curve represent the 3-loop perturbative QCD prediction.

3.2 Resummation of event shape variables

In this section we will give a brief introduction on the resummation formalism, following references [1] and [12].

We can begin by considering the perturbative prediction of the thrust distribution, which has the following form:

$$\frac{1}{\sigma}\frac{d\sigma}{dT} = \alpha_S(\mu^2)A_1(T) + \alpha_S^2(\mu^2)A_2(T, Q^2/\mu^2) + \alpha_S^3(\mu^2)A_3(T, Q^2/\mu^2) + ... \tag{3.16}$$

where $A_1(T)$ is given by Eq. (3.4).

The series expansion of a prediction is formally valid if $\alpha_S(\mu^2) \ll 1$; however, if the coefficients of the expansion are large, the prediction could lack reliability. For the thrust, as $T \to 1$, i.e. the final state reaches the 2-jet configuration, the coefficients become large, containing large logarithms:

$$A_n(T) \underset{T\to 1}{\sim} \frac{\log^{2n-1}(1-T)}{1-T}. \tag{3.17}$$

This means that the prediction is reliable only if $\alpha_S(\mu^2)\log^2(1-T) \ll 1$. A way to obtain a reliable prediction is to resum these large logarithms to all orders. For convenience, the resummation is performed considering the integrated distribution:

$$f(\tau) = \int_{1-\tau}^{1} dT \frac{1}{\sigma}\frac{d\sigma}{dT}, \tag{3.18}$$

where $\tau = 1 - T$. We say that the quantity exponentiates if for small values of τ it has the following form

$$f(\tau) = C(\alpha_S)\exp\left\{G\left(\alpha_S, \log\frac{1}{\tau}\right)\right\} + D(\alpha_S, \tau), \tag{3.19}$$

where, defining $L \equiv \log(1/\tau)$,

$$C(\alpha_S) = 1 + \sum_{n=1}^{+\infty} C_n \left(\frac{\alpha_S}{2\pi}\right)^n, \tag{3.20}$$

$$\begin{aligned} G(\alpha_S, L) &= \sum_{n=1}^{+\infty}\sum_{m=1}^{n+1} G_{nm}\left(\frac{\alpha_S}{2\pi}\right)^n L^m \\ &\equiv Lg_1(\alpha_S L) + g_2(\alpha_S L) + \alpha_S g_3(\alpha_S L) + ... \end{aligned} \tag{3.21}$$

$$D(\alpha_S, \tau) \underset{\tau\to 0}{\longrightarrow} 0. \tag{3.22}$$

We refer to terms $\alpha_S^n L^{n+1}$ as Leading Logarithms (LL), terms $\alpha_S^n L^n$ as Next-to-Leading Logarithms (NLL), and so on. The function g_1 resums all LL terms, g_2 all NLL terms, while g_3 and the next functions of the expansion contain the so-called subdominant logarithmic corrections $\alpha_S^n L^m$, with $0 < m < n$.

Knowing $g_1(\alpha_S L)$ and $g_2(\alpha_S L)$ in the region where $\alpha_S L \sim 1$, provided that the subdominant contributions have a good behaviour in this region, permits us to obtain a reliable prediction of $\log\tau$ in the region where $\alpha_S L \sim 1$, which is less limiting than the condition $\alpha_S L^2 \ll 1$.

We can say that every observable which is a solution of a RGE exponentiates. The exponentiation of an event shape is a consequence of the large logarithms arising from a large scale ratio in the calculation of the matrix elements in the infrared regions; however, the phase space may spoil this property. For the function $f(\tau)$ we can write

$$f(\tau) = \frac{1}{\sigma}\sum_n \int d\phi_n \left|\mathcal{M}_n\right|^2 F_n(\{p_i\}\,;\tau). \tag{3.23}$$

We have to show that each term of the sum factorize in the limit $\tau \to 0$, eventually after performing a suitable integral transformation; if the terms of the sum form an exponential series, we can say that the event shape exponentiates.

It can be shown that the thrust exponentiates; however, not all the event shape have this property. In general, an integrate distribution $R(v)$

$$R(v) = \frac{1}{\sigma}\int_0^v dv' \frac{d\sigma}{dv'}, \tag{3.24}$$

where $v \to 0$, has the following perturbative expansion:

$$R(v) = 1 + \sum_{n=1}^{+\infty}\left(\frac{\alpha_S}{2\pi}\right)^2\left(\sum_{m=1}^{2n} R_{nm}\log^m\frac{1}{v} + \mathcal{O}(v)\right). \tag{3.25}$$

In this case, reminding that $L \equiv \log(1/v)$, we refer to terms $\alpha_S^n L^{2n}$ as LL, terms $\alpha_S^n L^{2n-1}$ as NLL and so on. The resummation is convergent up to values for which $L \sim \alpha_S^{-1/2}$: beyond this limit, formally subleading terms can become as important as the leading terms. At this limit, a N^{n}LL resummation neglects terms of accuracy $\alpha_S^{(n+1)/2}$.

If the observable exponentiates, we can write

$$R(v) = \exp\left\{\sum_{n=1}^{+\infty}\left(\frac{\alpha_S}{2\pi}\right)^n\left(\sum_{m=0}^{n+1} G_{nm}\log^m\frac{1}{v} + \mathcal{O}(v)\right)\right\} \tag{3.26}$$

where the coefficients G_{nm} have the form of Eq. (3.21). It should be specified that we can rewrite every pertubative series in an exponential form: what distinguishes between an observable which exponentiates from a one which does not is the form of the coefficients G_{nm}.

Finally, it is worth spending some words about the matching between the fixed-order and resummed predictions. Resummed preditions are valid only in the limit of small v, while fixed-order calculations are performed in the whole phase space, but fail in a particular limit. Sometimes it could be useful to consider both these contributions; however, some terms are counted by both resummed and fixed-order calculations, so it is important to subtract the so-called double-counting terms. The matched prediction is

$$R^{\text{matched}}(v) = R^{\text{fixed-order}}(v) + R^{\text{resummed}}(v) - R^{\text{double-counting}}(v). \tag{3.27}$$

In the following plot, taken from [12], it is shown the difference between a fixed-order and a resummed predictions for the thrust.

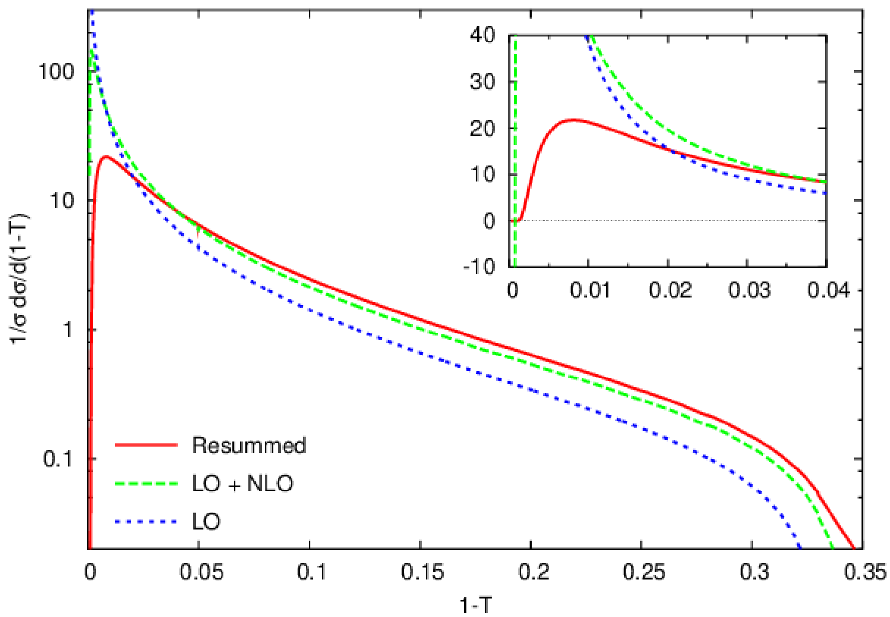

Figure 3.2: Comparison between fixed-order (LO, NLO) and resummed (NLL) predictions for the thrust distribution in electron-positron annihilation at $Q = M_Z$. The resummed prediction has been matched, so it contains LO and NLO contributions.

Chapter 4

Multifractals and renormalization in QFT

In this chapter we will give a brief introduction to the concept of multifractal. We will present the concept of a scaling law, a fractal system and its generalization to a multifractal system. Although these are concepts studied mainly in statistical physics, we will see that they have some application in QFT and QCD. We will see that a renormalizable quantum field theory has a multifractal behaviour.

4.1 Multifractals

We start by presenting the concept of multifractal: before doing this we will define a scaling law and a fractal system. The dissertation provided in this section is simple, having only the aim of introducing some basic concepts. Statistical physics literature is filled with works on these topics, but this goes beyond the aim of this thesis.

4.1.1 Scaling laws

A fundamental concept which is necessary to understand fractals and multifractals is the concept of scaling law. In general, a scaling law is a functional relation between two physical variables that depend on each other. A basic example is a power law:

$$f(x) = x^a, \tag{4.1}$$

where x is the independent variable, called scaling variable, and $a \in \mathbb{R}$. Typically, we take a length scale as scaling variable: a trivial example of a scaling power law is the dependence of the Coulomb force on the distance r:

$$F(r) \propto r^{-2}. \tag{4.2}$$

Physics is filled with scaling laws. In general, scaling laws can be more complicated than power laws; as we will see, fractals and multifractals are described by scaling laws.

4.1.2 Fractals

Conceptually, a fractal system is a system that repeats itself at every scale: this property is called self-similarity and it can be exact, approximate or statistical.

After hundreds of studies about fractals, in 1975 the mathematician Benoit Mandelbrot coined the word “fractal” and gave a mathematical definition supplied with computer-constructed visualizations, such as the so-called Mandelbrot set.

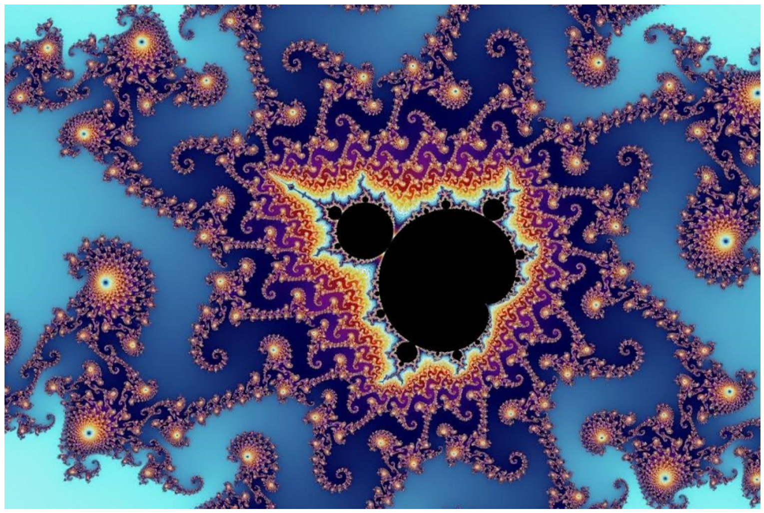

Figure 4.1: Visualization of a Mandelbrot set.

Mandelbrot describes a fractal as “a rough or fragmented geometric shape that can be split into parts, each of which is (at least approximately) a reduced size of the whole” [14]. A mathematical definition is provided introducing the concept of fractal dimension [15]: this measures how the detail in the fractal change with a change of the scale at which we are looking the system. The fractal dimension is greater than the topological dimension of the space. We consider a bounded set X in a d-dimensional space: X is self-similar if it is the union of N_r copies of itself, each of which is similar to X if scaled down by a factor r; the fractal dimension D_F is defined as follows:

$$D_F \equiv \frac{\log N_r}{\log \frac{1}{r}}. \tag{4.3}$$

In other words, we can imagine to divide the fractal space into hypercubes of side length r: if $N(r)$ is the number of hypercubes occupied by the points which form the fractal, we have that

$$D_F = -\lim_{r \to 0} \frac{\log N(r)}{\log r}. \tag{4.4}$$

Hence, fractals are described by a power scaling law, in which the power is minus the fractal dimension:

$$N(r) \propto r^{-D_F}. \tag{4.5}$$

Fractals appear in a variety of physical applications. For example, chaotic dynamical systems may exhibit a fractal behaviour.

4.1.3 Multifractals

A multifractal is the generalization of a fractal, which have a more than one fractal dimension or scaling rule. We can say that a fractal with a non-constant fractal dimension is a multifractal. In order to give a quantitative definition of a multifractal, we consider its application to dynamical systems following reference [16].

We consider a time series of points $X_i \equiv X(i\Delta t)$ of a dynamical system, where Δt is the time interval and $i = 1, 2, ..., N$:

$$\frac{d\mathbf{X}}{dt} = f(\mathbf{X}), \qquad\qquad \mathbf{X} \in \mathbb{R}^d. \tag{4.6}$$

We define a local density by counting the fraction of points contained in a hypersphere of radius r and centre X_i:

$$n_i(r) = \sum_{i \neq j} \frac{\Theta\left(r - |X_i - X_j|\right)}{N-1}, \tag{4.7}$$

where Θ is the Heaviside function. Through a space average we calculate the moments of this local density:

$$\langle n_i(r)^q \rangle = \lim_{N \to +\infty} \sum_{i=1}^{N} \frac{n_i(r)^q}{N}, \tag{4.8}$$

and define a series of exponents $\phi(q)$ by the scaling law

$$\lim_{r \to 0} \langle n_i(r)^q \rangle \propto r^{\phi(q)}. \tag{4.9}$$

In a fractal, $n(\lambda r)$ has the same statistical properties of $n(r)\lambda^{D_F}$, which implies that $\phi(q) = D_F q$. We have a multifractal if

$$\phi(q) \neq D_F q. \tag{4.10}$$

This idea can be generalized to a measure on a general d-dimensional space.

To sum up, while a fractal is a system that repeats itself at every scale, a multifractal is a system that, if looked at a different scale, repeats itself with some changes in its parameters.

4.2 Multifractal interpretation of the renormalization

In the first chapter we saw that higher-order corrections give rise to ultraviolet divergences, which are treated with the renormalization procedure. We saw that the renormalization of QCD requires a redefinition of the coupling constant: the consequence of this procedure is the introduction of a dependence of the coupling constant on an energy scale, called renormalization scale. This can be generalized to every renormalizable quantum field theory and to every parameter of the Lagrangian (masses, coupling constants, fields, etc.). Renormalizing a theory, we redefine the bare non-physical parameters of the Lagrangian at a certain energy scale. This means that we are looking at the system at a certain energy scale and we can wonder how the system changes if we observe it at a different scale.

Following chapter 12 of the reference [2], we illustrate this idea in the simple example of ϕ^4 theory, with a massless scalar field ϕ and a coupling constant λ. We start by introducing the bare Green's functions, defined as follows:

$$G_0^{(n)}(x_1, ..., x_n) = \langle 0|T\left\{\phi_0(x_1)\phi_0(x_2)...\phi_0(x_n)\right\}|0\rangle \, , \tag{4.11}$$

where T is the time-ordered product and ϕ_0 is the bare field. The Green's functions in Eq. (4.11) are functions of the bare coupling constant λ_0 and the UV cut-off Λ. After performing the renormalization, we remove the cut-off dependence, we substitute the bare coupling λ_0 with the renormalized coupling λ and rescale the fields introducing the field strength renormalization Z:

$$\phi(x) = Z^{-1/2}\phi_0(x). \tag{4.12}$$

The renormalized Green's functions $G^{(n)}(x_1, ..., x_n)$ depend on the renormalization scale μ and are numerically equal to the bare functions, up to a rescaling by powers of Z:

$$G^{(n)}(x_1, ..., x_n) = Z^{-n/2}G_0^{(n)}(x_1, ..., x_n). \tag{4.13}$$

We can redefine the renormalized Green's functions at a different scale μ', with a new renormalized coupling constant λ' and a new rescaling factor Z'. We consider an infinitesimal shift of the renormalization scale:

$$\begin{aligned} \mu &\to \mu + \delta\mu, & (4.14)\\ \lambda &\to \lambda + \delta\lambda, & (4.15)\\ \phi &\to (1+\delta\eta)\phi. & (4.16) \end{aligned}$$

This has the following effect on the renormalized Green's functions:

$$G^{(n)} \to (1 + n\delta\eta)G^{(n)}. \tag{4.17}$$

Thinking about $G^{(n)}$ as a function of M and λ, we can write

$$dG^{(n)} = \frac{\partial G^{(n)}}{\partial M}\delta M + \frac{\partial G^{(n)}}{\partial \lambda}\delta\lambda = n\delta\eta G^{(n)}. \tag{4.18}$$

It is useful to define the following dimensionless parameters:

$$\beta \equiv \frac{M}{\delta M}\delta\lambda, \qquad\qquad \gamma \equiv -\frac{M}{\delta M}\delta\eta. \tag{4.19}$$

Making these substitution in Eq. (4.18) and multiplying by $M/\delta M$, we obtain the following equation:

$$\left[\mu\frac{\partial}{\partial\mu} + \beta\frac{\partial}{\partial\lambda} + n\gamma\right]G^{(n)}(x_1, ..., x_n; \mu, \lambda) = 0. \tag{4.20}$$

The parameters β and γ are the same for every n and cannot depend on the x_i. Being $G^{(n)}$ renormalized, β and γ cannot depend on the cut-off, so, by dimensional analysis, we can conclude that they cannot depend on μ; hence, they are functions only of the dimensionless quantity λ. Therefore, we can say that any Green's function in massless ϕ^4 theory follows the so-called Callan-Symanzik equation:

$$\left[\mu\frac{\partial}{\partial\mu}+\beta(\lambda)\frac{\partial}{\partial\lambda}+n\gamma(\lambda)\right]G^{(n)}(x_1,...,x_n;\mu,\lambda)=0. \tag{4.21}$$

This result can be generalized to other renormalizable massless theory with dimensionless couplings. $\beta(\lambda)$ and $\gamma(\lambda)$ are two universal function: β has already been introduced in Chapter 1 and it is related to the coupling constant; whereas, $\gamma(\lambda)$ is called anomalous dimension and it is related to the operator we are rescaling (in this case the field).

We can conclude that, for a renormalizable theory, a shift in the renormalization scale leads to a shift in the coupling constant and in the other parameters of the Lagrangian. This means that, if we look at the system at a different energy scale, the system repeats itself with some changes in its parameters: remembering the definition given in the previous section, we can say that this is a multifractal behaviour.

4.2.1 Multifractals in QCD

Fractals and multifractals are a large field of interest in physics. Moreover, they have some applications in particle physics.

Some works about fractal and multifractal structures in multiparticle production are already available in literature. For example, the authors of [17] studied the multifractal dimensions in QCD cascades for high-energy particle production in small rapidity or angular intervals. A more recent work is [18], in which the authors present a series of fractal jet observables. However, in these and other works the common approach is to identify jets in the final state; our approach will be different: in the next chapter, we will calculate the multifractal dimension of a superinclusive observable at partonic level, without identifying jets.

Chapter 5

A superinclusive observable with a multifractal dimension

In this chapter we will define a superinclusive observable and we will study its behaviour in the collinear limit, through an analytical calculation at the Leading Log order. This chapter constitutes the original work of this thesis.

5.1 Definition of the observable

We consider an electron-positron scattering process e^+e^-, and, as done in Sect. 1.3.1, we make a calculation at LO in QED and consider the decay $\gamma \to q\bar{q}$ with QCD higher-order corrections; we neglect the Z channel. The observable is defined as the final-state energy deposited in a cone with angular radius θ:

$$E(\theta, b) \equiv \left(\sum_i E_i(\theta) \right)^b, \tag{5.1}$$

where $E_i(\theta)$ is the energy of the i-th particle revealed in the cone and b is a real parameter. This observable is superinclusive, since its definition is based on a property and not on the type of the final-state particles: we accept any possible final state.

5.1.1 Direction of the cone

Our aim is to find the behaviour of this variable in the limit where $\theta \to 0$. We should start by specifying the direction of the axis of the cone; we can explore different possibilities.

Direction of the LO quark-antiquark line

We can define the direction of the cone as the line of the quark-antiquark decay of the process at LO. This definition is particularly useful for analytical calculations, because the splitting angle of a parton emitted by the quark (or the antiquark) coincides with the angle between the parton and the cone axis; however, this has no sense experimentally, as we cannot identify the LO direction in an experiment.

Direction identified by the thrust axis

The thrust is a variable that identifies the direction which maximizes the longitudinal momentum of the final state. This direction can be determined in an experiment, but the calculations involved are not trivial.

Arbitrary direction

Another possibility is to choose an arbitrary direction in space as the direction of the cone axis. This has an experimental significance and the calculations can be simplified by a suitable choice of the frame of reference and the collinear approximation: in fact, we will see that in this limit we can approximate the direction of the cone with the direction of the LO quark-antiquark line in the phase-space regions which give a non-zero contribute to the observable.

Therefore, this is a good choice to study the scaling law of the observable. For convenience, we choose the frame of reference so that the z axis coincides with the axis of the cone: in this frame, a particle is inside the cone if and only if its polar angle is less than θ. Moreover, without loss of generality, we can set the azimuthal angle of the collision axis equal to zero; hence, in this frame the following four-vectors represents the initial-state four-momenta q_1 and q_2:

$$q_1 = (E, -E\sin\theta_0, 0, -E\cos\theta_0), \tag{5.2}$$
$$q_2 = (E, E\sin\theta_0, 0, E\cos\theta_0), \tag{5.3}$$

where we defined $E \equiv \frac{Q}{2} \equiv \frac{\sqrt{s}}{2}$, $\sqrt{s}$ being the centre-of-mass energy.

5.1.2 Formula of the observable for a n-particle final state

We can express the observable as a weighted cross section. We use the Heaviside function in order to say if a particle is inside or outside the cone: if it is outside, the function is equal to zero and it gives no contribution. For a general n-particle final state, we can write down the following formula:

$$E_n(\theta, b) = \frac{1}{2s\sigma_0}\int d\phi_n|\bar{\mathcal{M}}_n|^2\left(\sum_{i=1}^{n} E_i\Theta(\cos\theta_i - \cos\theta)\right)^b, \tag{5.4}$$

where $d\phi_n$ is the n-particle phase space and $|\bar{\mathcal{M}}_n|^2$ is the squared modulus of the $n-$particle final state amplitude (averaged over the polarizations); E_i and θ_i are the energy and the polar angle of the i-th particle respectively; $2s\sigma_0$ is a normalization factor, with σ_0 being the total cross section at Born level[1]. Finally, we define the following quantity, which will be useful in the calculations:

$$F_n(E_i, \theta_i; \theta, b) \equiv \left(\sum_{i=1}^{n} E_i\Theta(\cos\theta_i - \cos\theta)\right)^b \tag{5.5}$$

[1]Actually, a proper normalization would require the total cross section, but we approximate it using the Born-level one to make the calculations easier.

5.2 Fixed-order calculations

We will start by performing fixed-order calculations considering only leading logarithmic terms; then, we will sum the all-order contributions to obtain the LL result.

Fixed-order calculations can be performed by using Eq. (5.4); however, the integral could not be exactly calculable: in fact, if we consider the complete matrix element, we can compute the integral only at LO. Calculations are simpler in the soft and collinear limits, thanks to the factorization. As θ goes to zero, we are considering the collinear limit; we can also consider the soft limit, but we will see that the leading contributions to the variables are given by collinear partons and the collinear approximation is valid also if the emitted parton is soft.

5.2.1 LO calculation

At LO, we have the creations of a $q\bar{q}$ pair, with momenta p_1 and p_2 respectively:

$$\begin{aligned} p_1 &= (E_1, E_1 \sin\theta_1 \cos\varphi_1, E_1 \sin\theta_1 \sin\varphi_1, E_1 \cos\theta_1), && (5.6)\\ p_2 &= (E_2, E_2 \sin\theta_2 \cos\varphi_2, E_2 \sin\theta_2 \sin\varphi_2, E_2 \cos\theta_2). && (5.7) \end{aligned}$$

The conservation of the total four-momentum implies that

$$\begin{aligned} p_1 &= (E, E \sin\theta_1 \cos\varphi_1, E \sin\theta_1 \sin\varphi_1, E \cos\theta_1), && (5.8)\\ p_2 &= (E, -E \sin\theta_1 \cos\varphi_1, -E \sin\theta_1 \sin\varphi_1, -E \cos\theta_1). && (5.9) \end{aligned}$$

Inserting the expressions (5.2), (5.3) (5.8) and (5.9) into Eq. (1.24), we obtain the following result for the squared modulus of the amplitude at LO:

$$\begin{aligned} |\bar{\mathcal{M}}_{LO}|^2 &= \frac{8e^4 e_q^2}{(2E)^4}\left[E^4(1+\sin\theta_0\sin\theta_1\cos\varphi_1+\cos\theta_0\cos\theta_1)^2\right.\\ &\quad \left.+\,E^4(1-\sin\theta_0\sin\theta_1\cos\varphi_1-\cos\theta_0\cos\theta_1)^2\right]\\ &= \frac{8e^4 e_q^2 E^4}{16E^4}\left[2+2\sin^2\theta_0\sin^2\theta_1\cos^2\varphi_1+2\cos^2\theta_0\cos^2\theta_1\right.\\ &\quad \left.+4\sin\theta_0\sin\theta_1\cos\varphi_1\cos\theta_0\cos\theta_1\right]\\ &= e^4 e_q^2\left(1+\sin^2\theta_0\sin^2\theta_1\cos^2\varphi_1+\cos^2\theta_0\cos^2\theta_1\right.\\ &\quad \left.+\,2\sin\theta_0\cos\theta_0\sin\theta_1\cos\theta_1\cos\varphi_1\right). && (5.10) \end{aligned}$$

We can write down the expressions of the 2-particle phase space and of the quantity F_2:

$$d\phi_2 = d\Omega_1 \frac{1}{16\pi^2}\frac{|\mathbf{p}_1|}{Q} = \frac{1}{32\pi^2} d\cos\theta_1 d\varphi_1, \quad (5.11)$$

$$\begin{aligned} F_2(E_1,E_2,\theta_1,\theta_2;\theta,b) &= \left[E_1\Theta(\cos\theta_1-\cos\theta)+E_2\Theta(\cos\theta_2-\cos\theta)\right]^b\\ &= \left[E\Theta(\cos\theta_1-\cos\theta)+E\Theta(-\cos\theta_1-\cos\theta)\right]^b. && (5.12) \end{aligned}$$

The total cross section at Born level is given by eq. (1.26). Now, we can perform the computation of the observable at leading order, summing over all kinematically accessible flavours and all colours:

$$
\begin{aligned}
E_{LO}(\theta,b) &= \frac{3}{8\pi\alpha^2 N_c \sum_q e_q^2}\frac{N_c e^4 \sum_q e_q^2}{32\pi^2}\int_{-1}^{1} d\cos\theta_1 \int_0^{2\pi} d\varphi_1 (1+\sin^2\theta_0 \sin^2\theta_1 \cos^2\varphi_1 + \\
&\quad + \cos^2\theta_0\cos^2\theta_1 + 2\sin\theta_0\cos\theta_0\sin\theta_1\cos\theta_1\cos\varphi_1) F_2(E,\theta_1;\theta,b) \\
&= \frac{3}{8\pi\alpha^2}\frac{16\pi^2\alpha^2}{32\pi^2}\pi\int_{-1}^{1} d\cos\theta_1 (2+\sin^2\theta_1\sin^2\theta_0 + 2\cos^2\theta_1\cos^2\theta_0)\left[E\Theta(\cos\theta_1-\cos\theta)+\right. \\
&\quad \left. + E\Theta(-\cos\theta_1-\cos\theta)\right]^b \\
&= \frac{3}{16}E^b\left(\int_{\cos\theta}^{1} d\cos\theta_1(2+\sin^2\theta_1\sin^2\theta_0+2\cos^2\theta_1\cos^2\theta_0)+\right. \\
&\quad \left. + \int_{-1}^{-\cos\theta} d\cos\theta_1(2+\sin^2\theta_1\sin^2\theta_0+2\cos^2\theta_1\cos^2\theta_0)\right)
\end{aligned}
\tag{5.13}
$$

We focus on the first integral in Eq. (5.13) and compute it using the mean value theorem for integrals, considering that $\theta \ll 1$:

$$
\begin{aligned}
I_1 &\equiv \frac{3}{16}E^b\int_{\cos\theta}^{1} d\cos\theta_1(2+\sin^2\theta_1\sin^2\theta_0+2\cos^2\theta_1\cos^2\theta_0) \\
&= \frac{3}{16}E^b\int_0^{\theta} d\theta_1 \sin\theta_1(2+\sin^2\theta_1\sin^2\theta_0+2\cos^2\theta_1\cos^2\theta_0) \\
&= \frac{3}{16}E^b\theta\sin\frac{\theta}{2}(2+\sin^2\theta_0\sin^2\frac{\theta}{2}+2\cos^2\theta_0\cos^2\frac{\theta}{2})+\mathcal{O}(\theta^3) \\
&= \frac{3}{16}E^b\theta^2(1+\cos^2\theta_0)+\mathcal{O}(\theta^3).
\end{aligned}
\tag{5.14}
$$

The second integral in Eq. (5.13) is equal to the first: it can be seen by operating the substitution $\theta \to \pi - \theta$; the final result is the following:

$$
E_{LO}(\theta,b) = \frac{3}{8}E^b\theta^2(1+\cos^2\theta_0) \equiv C(\theta_0,b,E)\theta^2, \tag{5.15}
$$

where we have introduced the constant $C(\theta_0,b,E)$, which does not depend on θ, but only on fixed parameteres of the system:

$$
C(\theta_0,b,E) \equiv \frac{3}{8}E^b(1+\cos^2\theta_0). \tag{5.16}
$$

5.2.2 NLO calculation

At NLO we have the emission of a real or virtual gluon. We begin by considering the real emission: the partonic final state is $q\bar{q}g$ (see Fig. 1.3); using the notation of Section 1.3.1, we can write the expression of the observable at NLO:

$$
\begin{aligned}
E_{NLO}(\theta, q) &= \frac{1}{2s\sigma_0}\int d\phi_3 |\bar{\mathcal{M}}_0|^2 \left(E_1\Theta(\cos\theta_1 - \cos\theta) + E_2\Theta(\cos\theta_2 - \cos\theta)\right. \\
&\left. +E_3\Theta(\cos\theta_3 - \cos\theta)\right)^b , \qquad (5.17)
\end{aligned}
$$

where we have approximated the total cross section at NLO with the Born level total cross section.

In the collinear limit the interference between the two diagrams is suppressed and we can factorize the amplitude introducing the AP splitting functions:

$$
\int d\phi_3 |\bar{\mathcal{M}}_{NLO}|^2 = \int d\phi_2 |\bar{\mathcal{M}}_{LO}|^2 \frac{\alpha_S}{2\pi}\int \frac{dk_T^2}{k_T^2}\int dz P_{qq}^{(0)}(z), \qquad (5.18)
$$

where k_T is the transverse momentum of the gluon. From now on, we will refer to $P_{ab}^{(0)}(z)$ as $P_{ab}(z)$, because we will consider only the LO term of the AP functions. We start by considering the contribution given by the diagram (a), where the gluon is emitted by the quark; in the collinear approximation p_1 and p_2 have the same expression they have at LO.

$$
\begin{aligned}
E_{NLO}^{(a)}(\theta, b) &= \frac{\alpha_S}{2\pi}\frac{1}{2s\sigma_0}\int d\phi_2 |\bar{\mathcal{M}}_{LO}|^2 \int \frac{dk_T^2}{k_T^2}\int dz P_{qq}(z) \left[zE\Theta(\cos\theta_1 - \cos\theta) + \right. \\
&\left. + E\Theta(-\cos\theta_1 - \cos\theta) + (1-z)E\Theta(\cos\theta_3 - \cos\theta)\right]^b . \qquad (5.19)
\end{aligned}
$$

It's useful to split the integration domain into two regions, we can do that using the property of the Heaviside function:

$$
\begin{aligned}
E_{NLO}^{(a)}(\theta, b) &= \frac{\alpha_S}{2\pi}\int_{0\le\theta_1\le\theta} d\phi_2 \frac{|\bar{\mathcal{M}}_{LO}|^2}{2s\sigma_0} E^b \int \frac{d\theta_{13}^2}{\theta_{13}^2}\int dz P_{qq}(z) \left[z + (1-z)\Theta(\cos\theta_3 - \cos\theta)\right]^b + \\
&+ \frac{\alpha_S}{2\pi}\int_{\pi-\theta\le\theta_1\le\pi} d\phi_2 \frac{|\bar{\mathcal{M}}_{LO}|^2}{2s\sigma_0} E^b \int \frac{d\theta_{13}^2}{\theta_{13}^2}\int dz P_{qq}(z). \qquad (5.20)
\end{aligned}
$$

If $\pi - \theta \le \theta_1 \le \pi$, only the antiquark is revealed in the cone: considering also the virtual emission, this term gives no contribution, because of Eq. (2.31). As $\theta \ll 1$, we can use the approximation $\theta_{13} \approx \theta_3$:

$$
\begin{aligned}
E_{NLO}^{(a)}(\theta, b) &= \frac{\alpha_S}{2\pi}\int_{0\le\theta_1\le\theta} d\phi_2 \frac{|\bar{\mathcal{M}}_{LO}|^2}{2s\sigma_0} E^b \int_0^{\theta^2} \frac{d\theta_3^2}{\theta_3^2}\int dz P_{qq}(z) + \\
&+ \frac{\alpha_S}{2\pi}\int_{0\le\theta_1\le\theta} d\phi_2 \frac{|\bar{\mathcal{M}}_{LO}|^2}{2s\sigma_0} E^b \int_{\theta^2}^{\theta_m^2} \frac{d\theta_3^2}{\theta_3^2}\int dz P_{qq}(z) z^b, \qquad (5.21)
\end{aligned}
$$

where we have defined the angle $\theta_m > \theta$ as a superior limit of the collinear approximation. As before, the term containing the first momentum of $P_{qq}(z)$ vanishes.

$$
\begin{aligned}
E^{(a)}_{NLO}(\theta,b) &= \frac{\alpha_S}{2\pi}\int_{0\leq\theta_1\leq\theta} d\phi_2 \frac{|\bar{\mathcal{M}}_{LO}|^2}{2s\sigma_0} E^b \int_{\theta^2}^{\theta_m^2} \frac{d\theta_3^2}{\theta_3^2}\int dz P_{qq}(z) z^b \\
&= \frac{\alpha_S}{2\pi}\frac{1}{2} E_{LO}(\theta,b) 2\log\frac{\theta_m}{\theta}\int dz P_{qq}(z) z^b \\
&= \text{"not log"} - \frac{\alpha_S}{2\pi} E_{LO}(\theta,b)\left(\int dz P_{qq}(z) z^b\right)\log\theta \qquad (5.22)
\end{aligned}
$$

The contribution given by the diagram (b), $E^{(b)}_{NLO}(\theta,b)$, is equal to the one just computed:

$$
\begin{aligned}
E^{(b)}_{NLO}(\theta,b) &= \frac{\alpha_S}{2\pi}\frac{1}{2s\sigma_0}\int d\phi_2 |\bar{\mathcal{M}}_{LO}|^2 \int \frac{dk_T^2}{k_T^2}\int dz P_{qq}(z)[E\Theta(\cos\theta_1-\cos\theta)+ \\
&\quad +zE\Theta(-\cos\theta_1-\cos\theta)+(1-z)E\Theta(\cos\theta_3-\cos\theta)]^b \\
&= E^{(a)}_{NLO}(\theta,b). \qquad (5.23)
\end{aligned}
$$

Hence, the result is

$$
\begin{aligned}
E_{NLO}(\theta,b) &= \text{“not log”} - \frac{\alpha_S}{\pi} E_{LO}(\theta,b)\left(\int dz P_{qq}(z) z^b\right)\log\theta \\
&= \text{“not log”} - \frac{\alpha_S}{\pi} C(\theta_0,b,E)\theta^2\gamma_{qq}^{b+1}\log\theta, \qquad (5.24)
\end{aligned}
$$

where “not log” stands for non-logarithmic terms and γ_{qq} is the Mellin moment of the AP function $P_{qq}(z)$). Considering also the splitting $q\to g+q$ with its AP function $P_{gq}(z)$, the final result at NLO is the following:

$$
E_{NLO}(\theta,b) = -\frac{\alpha_S}{\pi} C(\theta_0,b,E)\theta^2\left(\gamma_{qq}^{b+1}+\gamma_{gq}^{b+1}\right)\log\theta, \qquad (5.25)
$$

which can be written also in a matrix form:

$$
\begin{aligned}
E_{NLO}(\theta,b) &= -\frac{\alpha_S}{\pi} C(\theta_0,b,E)\theta^2\log\theta\sum_{i=1}^{2}\left[\begin{pmatrix}\gamma_{qq}^{b+1} & 2N_f\gamma_{qg}^{b+1}\\ \gamma_{gq}^{b+1} & \gamma_{gg}^{b+1}\end{pmatrix}\cdot\begin{pmatrix}1\\0\end{pmatrix}\right]_i \\
&= -\frac{\alpha_S}{\pi} C(\theta_0,b,E)\theta^2\log\theta\sum_{i=1}^{2}\gamma_{ij}^{b+1}v_j, \qquad (5.26)
\end{aligned}
$$

where γ is the matrix whose elements are the Mellin moments of the AP functions, defined in Eq. (2.41, and $v_i\equiv(1,0)$ is the vector representing the initial state of the splitting process which contains one singlet quark and zero gluons. Being superinclusive, we consider the singlet distribution as we sum over all quarks and antiquarks flavours and sum the component of the final-state vector because we do not distinguish between quarks and gluons (the sum over j is understood).

In the generalization to the splitting $q \to g + q$, which leads to Eq. (5.25) we do not need the first Mellin moment of P_{gq} to be zero (indeed, it is not): if both the quark and the gluon are inside the cone, in fact, the splitting $q \to g + q$ can be seen as $q \to q + g$ in a different region of the phase space, as confirmed by the relation $P_{qq}(z) = P_{qg}(1 - z)$; hence, this term has already been taken into consideration, and its contribution to the observable vanishes since the first Mellin moment of P_{qq} is zero, as previously shown.

The final result at NLO order has a logarithmic dependence on the scale variable θ, which multiplies the quadratic term obtained at LO. It is worth noticing that the non-vanishing contributions are given by regions of the phase space where the the gluon is emitted outside the cone.

5.2.3 NNLO calculation

Now we calculate the expression of the variable with two collinear emissions. Firstly, we consider only the case of two gluon emissions, then we will generalize to all possible splittings. θ_3 and θ_4 are the emission angles respect to the quark direction, while z_3 and z_4 are the fraction of momentum transferred in the splitting processes. The Feynman diagrams are the following:

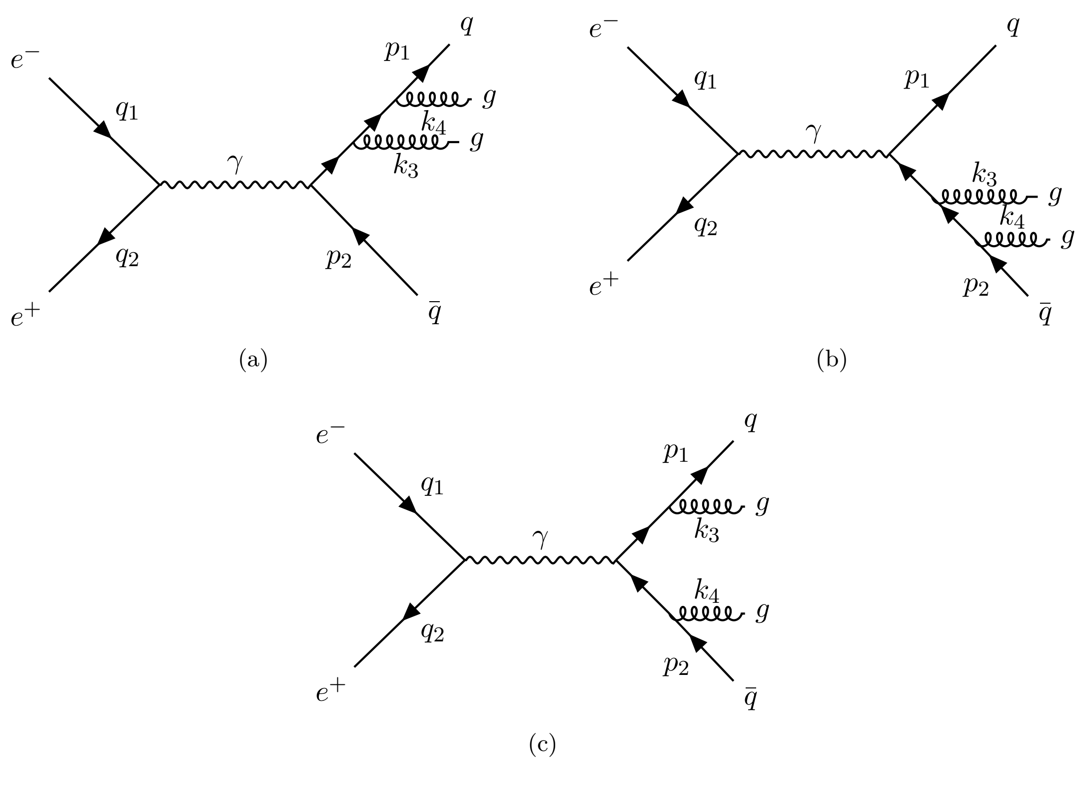

$$+ \ (3 \leftrightarrow 4)$$

Figure 5.1: Real emission Feynman diagrams of the process at NNLO.

We start by computing the contribution given by diagram (a):

$$
\begin{aligned}
E^{(a)}_{NNLO}(\theta,b) &= \frac{1}{2s\sigma_0}\int d\phi_2|\bar{\mathcal{M}}_{LO}|^2\frac{\alpha_S^2}{4\pi^2}\int\frac{dk_{3T}^2}{k_{3T}^2}\int\frac{dk_{4T}^2}{k_{4T}^2}\int dz_3P_{qq}(z_3)\int dz_4P_{qq}(z_4) \\
&\cdot[z_3z_4E\Theta(\cos\theta_1-\cos\theta)+E\Theta(-\cos\theta_1-\cos\theta) \\
&+(1-z_3)E\Theta(\cos\theta_3-\cos\theta)+z_3(1-z_4)E\Theta(\cos\theta_4-\cos\theta)]^b\,. \qquad (5.27)
\end{aligned}
$$

It can be shown that the leading contribution is given by the region where $0\le\theta_4\le\theta_3$:

$$
\begin{aligned}
E^{(a)}_{NNLO}(\theta,b) &= \int_{0\le\theta_1\le\theta}d\phi_2\frac{|\bar{\mathcal{M}}_{LO}|^2}{2s\sigma_0}E^b\frac{\alpha_S^2}{4\pi^2}\int_0^{\theta_m^2}\frac{d\theta_3^2}{\theta^2}\int_0^{\theta_3^2}\frac{d\theta_4^2}{\theta_4^2}\int dz_3P_{qq}(z_3)\int dz_4P_{qq}(z_4)[z_3z_4 \\
&+(1-z_3)\Theta(\cos\theta_3-\cos\theta)+z_3(1-z_4)\Theta(\cos\theta_4-\cos\theta)]^b \\
&+\int_{\pi-\theta\le\theta_1\le\pi}d\phi_2\frac{|\bar{\mathcal{M}}_{LO}|^2}{2s\sigma_0}E^b\frac{\alpha_S^2}{4\pi^2}\int_0^{\theta_m^2}\frac{d\theta_3^2}{\theta^2}\int_0^{\theta_3^2}\frac{d\theta_4^2}{\theta_4^2}\int dz_3P_{qq}(z_3)\int dz_4P_{qq}(z_4), \qquad (5.28)
\end{aligned}
$$

As before, the region $\pi-\theta\le\theta_1\le\pi$ gives no contribution:

$$
\begin{aligned}
E^{(a)}_{NNLO}(\theta,b) &= \frac{\alpha_S^2}{4\pi^2}\frac{1}{2}E_{LO}(\theta,b)\int_0^{\theta^2}\frac{d\theta_3^2}{\theta^2}\int_0^{\theta_3^2}\frac{d\theta_4^2}{\theta_4^2}\int dz_3P_{qq}(z_3)\int dz_4P_{qq}(z_4) \\
&\cdot[z_3z_4+(1-z_3)+z_3(1-z_4)]^b \\
&+\frac{\alpha_S^2}{4\pi^2}\frac{1}{2}E_{LO}(\theta,b)\int_{\theta^2}^{\theta_m^2}\frac{d\theta_3^2}{\theta^2}\int_0^{\theta^2}\frac{d\theta_4^2}{\theta_4^2}\int dz_3P_{qq}(z_3)\int dz_4P_{qq}(z_4) \\
&\cdot[z_3z_4+z_3(1-z_4)]^b \\
&+\frac{\alpha_S^2}{4\pi^2}\frac{1}{2}E_{LO}(\theta,b)\int_{\theta^2}^{\theta_m^2}\frac{d\theta_3^2}{\theta^2}\int_{\theta^2}^{\theta_3^2}\frac{d\theta_4^2}{\theta_4^2}\int dz_3P_{qq}(z_3)\int dz_4P_{qq}(z_4)[z_3z_4]^b. \qquad (5.29)
\end{aligned}
$$

Only the last integral survives, since

$$
z_3z_4+(1-z_3)+z_3(1-z_4)=1, \qquad\qquad z_3z_4+z_3(1-z_4)=z_3. \qquad (5.30)
$$

The phase-space integral gives the following result:

$$
\begin{aligned}
\int_{\theta^2}^{\theta_m^2}\frac{d\theta_3^2}{\theta^2}\int_{\theta^2}^{\theta_3^2}\frac{d\theta_4^2}{\theta_4^2} &= \int_{\theta^2}^{\theta_m^2}\left(\log\theta_3^2-\log\theta^2\right)^2 \\
&= \frac{1}{2}\left(\log\theta_m^2-\log\theta^2\right)^2 \\
&= \frac{1}{2}\log\theta^2+\mathcal{O}(\log\theta) \qquad (5.31)
\end{aligned}
$$

Therefore, we can notice that the only region of the phase space that gives a non-vanishing contribution is the one where both the gluons are emitted outside the cone. The result has a quadratic dependence on the logarithm of θ, diagram (b) gives the same contribution, while diagram (c) gives a lower-order logarithmic term. The result is the following:

$$
\begin{aligned}
E_{NNLO}(\theta,b) &= 2\frac{\alpha_S^2}{4\pi^2}\frac{1}{2}E_{LO}(\theta,b)\frac{1}{2}\left(\log\theta_m^2-\log\theta^2\right)^2\int dz_3 P_{qq}(z_3)z_3^b\int dz_4 P_{qq}(z_4)z_4^b+\mathcal{O}(\log\theta)\\
&= \frac{1}{2}\frac{\alpha_S^2}{4\pi^2}E_{LO}(\theta,b)4\log^2\theta\left(\gamma_{qq}^{b+1}\right)^2+\mathcal{O}(\log\theta)\\
&= \frac{1}{2}\left(-\frac{\alpha_S}{\pi}\right)^2 C(\theta_0,b,E)\theta^2\log^2\theta\left(\gamma_{qq}^{b+1}\right)^2+\mathcal{O}(\log\theta). \qquad (5.32)
\end{aligned}
$$

Now, we can consider all possible splittings:

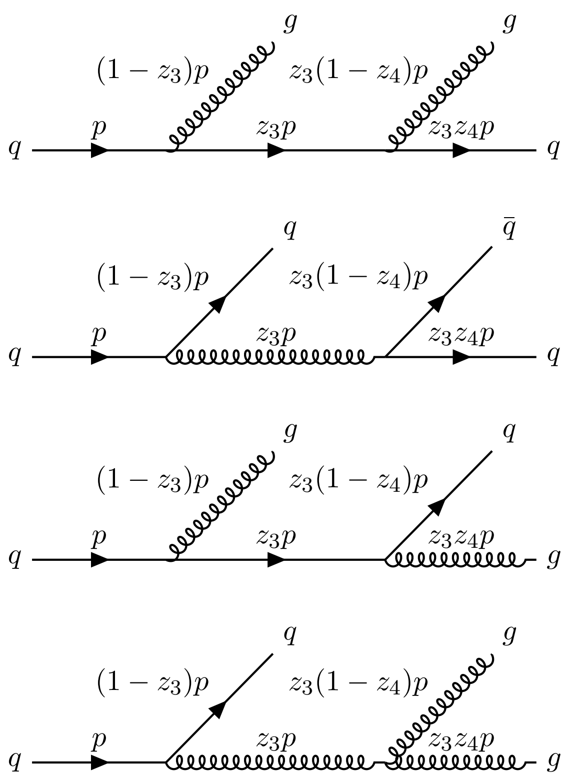

$\Longrightarrow \quad P_{qg}(z_4)P_{gq}(z_3),$

$\Longrightarrow \quad P_{qg}(z_4)P_{gq}(z_3),$

$\Longrightarrow \quad P_{gq}(z_4)P_{qq}(z_3),$

$\Longrightarrow \quad P_{gg}(z_4)P_{gq}(z_3).$

Figure 5.2: Possible splittings and related Altarelli-Parisi functions for the process at NLO.

We obtain the following expression:

$$
\begin{aligned}
E_{NNLO}(\theta,b) &= \frac{1}{2}\left(-\frac{\alpha_S}{\pi}\right)^2 C(\theta_0,b,E)\theta^2\log^2\theta\left[\left(\gamma_{qq}^{b+1}\right)^2+2N_f\gamma_{qg}^{b+1}\gamma_{gq}^{b+1}\right.\\
&\quad\left.+\gamma_{gq}^{b+1}\gamma_{qq}^{b+1}+\gamma_{gg}^{b+1}\gamma_{gq}^{b+1}\right]+\mathcal{O}(\log\theta), \qquad (5.33)
\end{aligned}
$$

which can be written in a matrix form:

$$\begin{aligned}
E_{NNLO}(\theta,b) &= \frac{1}{2}\left(-\frac{\alpha_S}{\pi}\right)^2 C(\theta_0,b,E)\theta^2\log^2\theta\sum_{i=1}^{2}\gamma_{ij}^{b+1}\gamma_{jk}^{b+1}v_k+\mathcal{O}(\log\theta)\\
&= \frac{1}{2}\left(-\frac{\alpha_S}{\pi}\right)^2 C(\theta_0,b,E)\theta^2\log^2\theta\sum_{i=1}^{2}\left[\left(\gamma^{b+1}\right)^2\right]_{ij}v_j+\mathcal{O}(\log\theta) \qquad (5.34)
\end{aligned}$$

in fact

$$\begin{aligned}
&\begin{pmatrix}\gamma_{qq}^{b+1} & 2N_f\gamma_{qg}^{b+1}\\ \gamma_{gq}^{b+1} & \gamma_{gg}^{b+1}\end{pmatrix}\cdot\begin{pmatrix}\gamma_{qq}^{b+1} & 2N_f\gamma_{qg}^{b+1}\\ \gamma_{gq}^{b+1} & \gamma_{gg}^{b+1}\end{pmatrix}\cdot\begin{pmatrix}1\\0\end{pmatrix}=\begin{pmatrix}\gamma_{qq}^{b+1} & 2N_f\gamma_{qg}^{b+1}\\ \gamma_{gq}^{b+1} & \gamma_{gg}^{b+1}\end{pmatrix}\cdot\begin{pmatrix}\gamma_{qq}^{b+1}\\ \gamma_{gq}^{b+1}\end{pmatrix}=\\
&=\begin{pmatrix}\left(\gamma_{qq}^{b+1}\right)^2+2N_f\gamma_{qg}^{b+1}\gamma_{gq}^{b+1}\\ \gamma_{gq}^{b+1}\gamma_{qq}^{b+1}+\gamma_{gg}^{b+1}\gamma_{gq}^{b+1}\end{pmatrix}\\
\Rightarrow\quad &\sum_{i=1}^{2}\left[\left(\gamma^{b+1}\right)^2\right]_{ij}v_j=\left(\gamma_{qq}^{b+1}\right)^2+2N_f\gamma_{qg}^{b+1}\gamma_{gq}^{b+1}+\gamma_{gq}^{b+1}\gamma_{qq}^{b+1}+\gamma_{gg}^{b+1}\gamma_{gq}^{b+1} \qquad (5.35)
\end{aligned}$$

and we obtain the expression of Eq. (5.33).

5.2.4 N^{n}LO calculation

We can generalize these results to the case of n emissions. We begin by considering the emission of n gluons, with angles $\theta_3,\theta_4,...,\theta_{n+3}$; the Leading Log term is given by the diagram in which all the gluons come from the same quark line, multiplied by 2 because at LO we have two quarks line; the phase-space region which gives a non-vanishing contribute is the one where all the gluons are outside the cone.

$$E_{N^nLO}(\theta,b)=2\left(\frac{\alpha_S}{2\pi}\right)^n\frac{1}{2}E_{LO}(\theta,b)I_n\int dz_3P_{qq}(z_3)\int dz_4P_{qq}(z_4)...\int dz_{n+3}P_{qq}(z_{n+3})[z_3z_4...z_{n+3}]^b, \qquad (5.36)$$

where I_n is the following angular integral, whose the result is the generalization of the one obtained for $n=2$:

$$\begin{aligned}
I_n &= \int_{\theta^2}^{\theta_m^2}\frac{d\theta_3^2}{\theta_3^2}\int_{\theta^2}^{\theta_3^2}\frac{d\theta_4^2}{\theta_4^2}\cdot...\cdot\int_{\theta^2}^{\theta_{n+2}^2}\frac{d\theta_{n+3}^2}{\theta_{n+3}^2}=\frac{1}{n!}(\log\theta_m^2-\log\theta^2)^n\\
&= \frac{(-1)^n}{n!}\log^n\theta^2+\mathcal{O}(\log^{n-1}\theta)=\frac{(-1)^n}{n!}2^n\log^n\theta+\mathcal{O}(\log^{n-1}\theta). \qquad (5.37)
\end{aligned}$$

So

$$
\begin{aligned}
E_{N^nLO}(\theta,b) &= \left(\frac{\alpha_S}{2\pi}\right)^n E_{LO}(\theta,b)\frac{(-1)^n}{n!}2^n\log^n\theta\left(\int dz P(z)z^b\right)^n + \mathcal{O}(\log^{n-1}\theta) \\
&= \frac{1}{n!}\left(-\frac{\alpha_S}{\pi}\right)^n C(\theta_0,b,E)\theta^2\log^n\theta\left(\gamma_{qq}^{b+1}\right)^n + \mathcal{O}(\log^{n-1}\theta). \qquad (5.38)
\end{aligned}
$$

Generalizing to any possible splitting the result is the following:

$$
E_{N^nLO}(\theta,b) = \frac{1}{n!}\left(-\frac{\alpha_S}{\pi}\right)^n C(\theta_0,b,E)\theta^2\log^n\theta\sum_{i=1}^{2}\left[\left(\gamma^{b+1}\right)^n\right]_{ij} v_j + \mathcal{O}(\log^{n-1}\theta). \qquad (5.39)
$$

We can prove the validity of Eq. (5.39) by induction. The inductive hypothesis is that the formula is valid at order $n-1$: at this order, the diagrams which give Leading Log contributes are the ones with $n-1$ emissions from the same quark line, which can end with a quark or a gluon; if it ends with a quark, the n-th emission could be $q \to qg$ ($P_{qq}(z)$) or $q \to gq$ ($P_{gq}(z)$); instead, if the line ends with a gluon, the n-th emission could be $g \to gg$ ($P_{gg}(z)$) or $g \to q\bar{q}$ ($P_{qg}(z)$). In order to calculate the amplitude, we should distinguish these cases and multiply by the related AP functions, which mathematically means multiplying the splitting matrix by the state vector after $n-1$ emissions, which is equal to $\left[\left(\gamma^{b+1}\right)^{n-1}\right]_{ij} v_j$ for the inductive hypothesis: thus, it is clear that the state vector after n emissions is equal to $\left[\left(\gamma^{b+1}\right)^n\right]_{ij} v_j$. Calculating the prediction of the observable, we don't distinguish between different final states, so we should sum the components of the vector.

5.3 Resummation of LL terms

After computing fixed-order calculations, we notice that the result can be resummed, obtaining the Leading-Log prediction:

$$
\begin{aligned}
E_{LL}(\theta,b) &= \sum_{n=0}^{+\infty}\frac{1}{n!}\left(-\frac{\alpha_S}{\pi}\right)^n C(\theta_0,b,E)\theta^2\log^n\theta\sum_{i=1}^{2}\left[\left(\gamma^{b+1}\right)^n\right]_{ij} v_j \\
&= C(\theta_0,b,E)\theta^2\sum_{i=1}^{2}\left[\sum_{n=0}^{+\infty}\frac{1}{n!}\left(-\frac{\alpha_S}{\pi}\log\theta\right)^n\left(\gamma^{b+1}\right)^n\right]_{ij} v_j \\
&= C(\theta_0,b,E)\theta^2\sum_{i=1}^{2}\left[e^{-\alpha_S/\pi\log\theta\left(\gamma^{b+1}\right)}\right]_{ij} v_j \\
&= C(\theta_0,b,E)\theta^2\sum_{i=1}^{2}\left[\theta^{-\alpha_S/\pi\left(\gamma^{b+1}\right)}\right]_{ij} v_j \\
&\equiv C(\theta_0,b,E)\sum_{i=1}^{2}\left[\theta^{\phi(b)}\right]_{ij} v_j. \qquad (5.40)
\end{aligned}
$$

Being θ the scale variable, the observable follows a scaling law similar to Eq. (4.9). Hence, we obtain a multifractal law with dimension $\phi(b)$, given by the following expression:

$$\phi_{ij}(b) \equiv 2\delta_{ij} - \frac{\alpha_S}{\pi}\left(\gamma^{b+1}\right)_{ij} \tag{5.41}$$

5.4 Running coupling constant

The result is different if we consider the running coupling: in particular, the angular integral changes, while the factors containing the moments of the AP functions remain the same. For n emissions we have

$$E_n(\theta, b) = 2 \cdot \left(\frac{1}{2\pi}\right)^n \frac{1}{2} E_{LO}(\theta, b) \tilde{I}_n \sum_{i=1}^{2} \left[\left(\gamma^{b+1}\right)^n\right]_{ij} v_j, \tag{5.42}$$

where

$$\tilde{I}_n = \int_{\theta^2}^{\theta_m^2} \frac{d\theta_3^2}{\theta_3^2} \alpha_S(\theta_3^2 E^2) \int_{\theta^2}^{\theta_3^2} \frac{d\theta_4^2}{\theta_4^2} \alpha_S(\theta_4^2 E^2) \cdot \ldots \cdot \int_{\theta^2}^{\theta_{n+2}^2} \frac{d\theta_{n+3}^2}{\theta_{n+3}^2} \alpha_S(\theta_{n+3}^2 E^2). \tag{5.43}$$

Using Eq. (1.18) and Eq. (1.23), we can express the running coupling constant at the energy θE:

$$\alpha_S(\theta^2 E^2) = \frac{\alpha_S(\mu^2)}{1 + \beta_0 \alpha_S(\mu^2) \log \frac{\theta^2 E^2}{\mu^2}} = \frac{1}{\beta_0 \log \frac{\theta^2 E^2}{\Lambda^2}} \tag{5.44}$$

where μ is the renormalization scale and $\Lambda \equiv \Lambda_{QCD}$. We start by calculating $\tilde{I}_n$:

$$\begin{aligned}
\int_{\theta^2}^{\theta_{n+2}^2} \frac{d\theta_{n+3}^2}{\theta_{n+3}^2} \alpha_S(\theta_{n+3}^2 E^2) &= \frac{1}{\beta_0} \int_{\theta^2}^{\theta_{n+2}^2} \frac{d\theta_{n+3}^2}{\theta_{n+3}^2} \frac{1}{\log \frac{\theta_{n+3}^2 E^2}{\Lambda^2}} \\
&= \frac{1}{\beta_0} \left[\log\left(\log \frac{\theta_{n+2}^2 E^2}{\Lambda^2}\right) - \log\left(\log \frac{\theta^2 E^2}{\Lambda^2}\right)\right],
\end{aligned} \tag{5.45}$$

$$\begin{aligned}
\int_{\theta^2}^{\theta_{n+1}^2} \alpha_S(\theta_{n+2}^2 E^2) \int_{\theta^2}^{\theta_{n+2}^2} \frac{d\theta_{n+3}^2}{\theta_{n+3}^2} \alpha_S(\theta_{n+3}^2 E^2) &= \frac{1}{\beta_0^2} \int_{\theta^2}^{\theta_{n+1}^2} \frac{d\theta_{n+2}^2}{\theta_{n+2}^2} \frac{1}{\log \frac{\theta_{n+2}^2 E^2}{\Lambda^2}} \left[\log\left(\log \frac{\theta_{n+2}^2 E^2}{\Lambda^2}\right)\right. \\
&\quad \left. - \log\left(\frac{\theta^2 E^2}{\Lambda^2}\right)\right] \\
&= \frac{1}{2}\frac{1}{\beta_0^2} \left[\log\left(\log \frac{\theta_{n+1}^2 E^2}{\Lambda^2}\right) - \log\left(\log \frac{\theta^2 E^2}{\Lambda^2}\right)\right]^2.
\end{aligned} \tag{5.46}$$

After n steps we obtain

$$
\begin{aligned}
\tilde{I}_n &= \frac{1}{n!}\frac{1}{\beta_0^n}\left[\log\left(\frac{1+\beta_0\alpha_S(\mu^2)\log\frac{\theta_m^2E^2}{\mu^2}}{\beta_0\alpha_S(\mu^2)}\right)-\log\left(\frac{1+\beta_0\alpha_S(\mu^2)\log\frac{\theta^2E^2}{\mu^2}}{\beta_0\alpha_S(\mu^2)}\right)\right]^n \\
&= \frac{1}{n!}\frac{(-1)^n}{\beta_0^n}\log^n\left(\frac{1+2\beta_0\alpha_S(\mu^2)\log\frac{\theta E}{\mu}}{1+2\beta_0\alpha_S(\mu^2)\log\frac{\theta_m E}{\mu}}\right) \\
&= \frac{1}{n!}\frac{(-1)^n}{\beta_0^n}\log^n\left(1+2\beta_0\alpha_S(\mu^2)\log\frac{\theta E}{\mu}\right)+\mathcal{O}\left(NLL\right). \qquad (5.47)
\end{aligned}
$$

So Eq. (5.42) becomes

$$
E_n(\theta,b)=\frac{1}{n!}\left(-\frac{1}{2\pi\beta_0}\right)^n C(\theta_0,b,E)\theta^2\log^n\left(1+2\beta_0\alpha_S(\mu^2)\log\frac{\theta E}{\mu}\right)\sum_{i=1}^{2}\left[\left(\gamma^{b+1}\right)^n\right]_{ij}v_j. \quad (5.48)
$$

It should be specified that in this case θ can't be arbitrary small, but it has to be greater than a limit value, which depends on the Landau pole of QCD:

$$
\theta>\frac{\mu}{E}\exp\left(-\frac{1}{2\beta_0\alpha_S(\mu^2)}\right)=\frac{\Lambda}{E}. \qquad (5.49)
$$

Now, we can resum the LL terms:

$$
\begin{aligned}
E_{LL}(\theta,b) &= \sum_{n=0}^{+\infty}\frac{1}{n!}\left(-\frac{1}{2\pi\beta_0}\right)^n C(\theta_0,b,E)\theta^2\log^n\left(1+2\beta_0\alpha_S(\mu^2)\log\frac{\theta E}{\mu}\right)\sum_{i=1}^{2}\left[\left(\gamma^{b+1}\right)^n\right]_{ij}v_j \\
&= C(\theta_0,b,E)\theta^2\sum_{i=1}^{2}\left[\sum_{n=0}^{+\infty}\frac{1}{n!}\left(-\frac{1}{2\pi\beta_0}\log\left(1+2\beta_0\alpha_S(\mu^2)\log\frac{\theta E}{\mu}\right)\right)^n\left(\gamma^{b+1}\right)^n\right]_{ij}v_j \\
&= C(\theta_0,b,E)\theta^2\sum_{i=1}^{2}\left[\exp\left\{-\frac{1}{2\pi\beta_0}\log\left(1+2\beta_0\alpha_S(\mu^2)\log\frac{\theta E}{\mu}\right)\left(\gamma^{b+1}\right)\right\}\right]_{ij}v_j \\
&= C(\theta_0,b,E)\theta^2\sum_{i=1}^{2}\left[\left(1+2\beta_0\alpha_S(\mu^2)\log\frac{\theta E}{\mu}\right)^{-1/(2\pi\beta_0)\left(\gamma^{b+1}\right)}\right]_{ij}v_j. \qquad (5.50)
\end{aligned}
$$

With the running coupling constant, the scaling law is different: we have a function of $\log\theta$ instead of θ playing the role of the scaling variable and also the multifractal dimension is different: it does not contain α_S, but the information about the coupling enters through β_0.

Chapter 6

Interpretation of the results and conclusions

After performing a LL calculation, we proved that the superinclusive observable follows a multifractal law. Now, we present some considerations:

- the scaling law is a direct consequence of the presence of collinear logarithms;
- the non-vanishing contributes to the observable come from particles emitted outside the cone;
- the multifractal dimension contains the anomalous dimension of the Altarelli-Parisi splitting functions;
- although with different law, the multifractal behaviour is still present if we consider the running coupling constant;
- we performed a partonic calculation without identifying jets in the final state.

We can say that this law may represent an expression of the multifractal nature of QCD.

It is important to remember that we verified the multifractal law only with a LL calculation. This result could be improved generalizing the calculation at N^{n}LL and studying the parton-hadron duality of this observable, eventually comparing the prediction with Monte-Carlo simulations.

The authors of [13] made a similar calculation at partonic level for conformal theories, at all orders. Most recent works focus on correlators inside jets, finding power laws similar to the one obtained in this thesis. However, as we said before, EEC are widely-used variables: the innovative approach of the work in this thesis is the fact that we considered a general final state without identifying jets.

If we demonstrate that the parton-hadron duality is valid for this observable, we could use it in order to obtain a measure of the running coupling constant: in fact, the observable can be measured experimentally, measuring the energy of the particles inside the cone, and, if the parton-hadron duality is valid, we can compare this measurement with the theoretical prediction and measure the running coupling constant, as the prediction will depend on α_S. An advantage of this method is that this measurement will not require the use of PDFs.

Bibliography

[1] R. K. Ellis, W. J. Stirling, B. R. Webber, *QCD and Collider Physics*.

[2] M. E. Peskin, D. V. Schroeder, *An Introduction to Quantum Field Theory*.

[3] G. Parisi, *Superinclusive cross sections*, January 1978.

[4] G. Altarelli, G. Parisi, *Asymptotic freedom in parton language*, 12 April 1977.

[5] G. Parisi, R. Petronzio, *On the breaking of Bjorken scaling*, 25 March 1976.

[6] D. J. Gross, F. Wilczek, *Asymptotically free gauge theories. II*, 27 August 1973.

[7] G. Luisoni, S. Marzani, *QCD resummation for hadronic final states*, arXiv:1505.04084v3 [hep-ph] 10 Oct 2017.

[8] S. Marzani, G. Soyez, M. Spannowsky, *Looking inside jets: an introduction to jet substructure and boosted-object phenomenology*, arXiv:1505.04084v3 [hep-ph] 10 Oct 2017.

[9] OPAL Collaboration, P.D. Acton, et al., *Z. Phys. C*, **55** (1992), p. 1

[10] K. Nakamura et al., *J. Phys.*, **G37** (2010) 075021; http://pdg.lbl.gov/

[11] A. Pich, *The Standard Model of Electroweak Interactions*, arXiv:1201.0537v1 [hep-ph] 2 Jan 2012.

[12] M. Dasgupta, G. P. Salam, *Event shapes in* e^+e^- *annihilation and deep inelastic scattering*, arXiv:0312283v2 [hep-ph] 2 Jan 2004.

[13] D. F. Hofman, J. Maldacena, *Conformal collider physics: energy and charge correlators*, arXiv:0803.1467v3 [hep-th] 4 May 2008.

[14] B. Mandelbrot, *The fractal geometry of nature*, 1984.

[15] B. Mandelbrot, *How Long Is the Coast of Britain? Statistical Self-Similarity and Fractional Dimension*, *Science*, New Series, Vol. 156, No. 3775, 5 May 1967.

[16] R. Benzi et al., *J. Phys. A: Math. Gen.* **17** (1984) 3521.

[17] G. Gustafson and A. Nilsson, *Multifractal dimensions in QCD cascades*, 15 April 1991.

[18] B. T. Elder, M. Procura, J. Thaler, W. J. Waalewijn and K. Zhou, *Generalized Fragmentation Functions for Fractal Jet Observables*, arXiv:1704.05456v1 [hep-ph] 18 Apr 2017.